Designing and testing a microfluidic chip for monitoring stimulated cells with a biosensor

van Slagmaat, L.M.

Award date:
2021

Eindhoven University of Technology

Designing and testing a microfluidic chip for monitoring stimulated cells with a biosensor

Final report of the Master Graduation Project

This report was made in accordance with the TU/e Code of Scientific Conduct for the Master thesis

Lisa van Slagmaat 0857566
Supervisors:
Dr. L.J. van IJzendoorn
Prof. J.M.J. den Toonder
MSc. M.H. Bergkamp

Eindhoven, October 31, 2021

Declaration concerning the TU/e Code of Scientific Conduct

I have read the TU/e Code of Scientific Conduct[i].

In carrying out research, design and educational activities, I shall observe the five central values of scientific integrity, namely: trustworthiness, intellectual honesty, openness, independence and societal responsibility, as well as the norms and principles which follow from them.

Date

31 October 2021

Name

Lisa van Slagmaat

ID-number

0857566

Signature

Submit the signed declaration to the student administration of your department.

[i] See: https://www.tue.nl/en/our-university/about-the-university/organization/integrity/scientific-integrity/
The Netherlands Code of Conduct for Scientific Integrity, endorsed by 6 umbrella organizations, including the VSNU, can be found here also. More information about scientific integrity is published on the websites of TU/e and VSNU

Abstract

Advances in the field of microfluidics in the last decades have enabled the integration of cell culture in microfluidic devices, which lead to the development of "organ-on-a-chip". This technology utilises representative models of physiology in the form of 3D multicellular microtissues or organoids in microfluidic devices to study biological processes [1]. Although the technology is still in its infancy [2], physiologically relevant models with integrated biosensors are promising to both medical research and healthcare [3]. They could be used to replace animal models and traditional cell culture for disease modelling or drug screening. Additionally, they could be used in personalized medicine, creating a model of a patient to diagnose and investigate treatment options. In cancer research, information about cell metabolism can characterize tumor development and can be used to screen drugs [3].

In this context, this project aims to develop a microfluidic device to probe the production of IL-6, a cytokine involved in the inflammatory response, of triple negative MDA MB 231 breast cancer cells as a response to stimulation with TNF-α.

The microfluidic devices of this project were made using PDMS soft-lithography and sandwich immunoassay techniques were used for the biosensing components of this work. Stimulated IL-6 production in traditional cell culture vessels and basal production of the MDA MB 231 cell line were both in accordance with literature. [4] [5] Control experiments with MCF 7 cells yielded no detectable IL-6 as expected. The proposed microfluidic chip contains a novel bolt-nut valve design to close off separate chambers, the functioning of which was tested and determined to be adequate for flows from 10 μL/min to 5 mL/min, which is amply sufficient for the proposed use. The cell viability in the device was above 97%, similar to that of a well plate. The limit of detection of a fluorescent assay was determined to be 5 $\pm$0,2 nM, which is not sufficient to measure the produced IL-6 concentration range of 450pM in a chip. The rate of production of IL-6 per cell inside the microfluidic device was found to be in accordance with prior experiments in traditional cell culture vessels.

Recommendations for further research include: using cell cultures with low passage count; applying methods to achieve homogeneous and precise cell counts upon seeding, such as automated cell counting to improve reproduciblility; and improving the optical setup, in particular the camera, to increase the sensitivity of the sensing method.
Overall, the results of the design are promising. After the implementation of the recommendations, a fully functioning device seems possible.

Acknowledgements

Research projects are always teamwork, my graduation project included. As such, I have many people to thank for their help.

I would like to thank my supervisors Leo van Ijzendoorn, Jaap den Toonder, and Max Bergkamp for the continued coaching and guidance they provided across the whole length of the project. Thank you for giving me the opportunity to pursue my interests in the form of this project.

I thank my boyfriend for supporting me outside of my work on this project and always taking the time to help and encourage me, especially during busy times.

I am grateful to Hulan Sergelen for assisting and guiding me through my first biochemical experiments, for helping me become a competent experimentalist in a biochemical lab, and finally for her career advice.

I would like to thank Laura Woythe for teaching me cell culture techniques, essential to my project, and for patiently sharing her biology knowledge with me, someone who had never seen a well plate until almost a year ago.

I thank Zhiwei Cui for introducing me to the lithography techniques, the core of microfluidic device fabrication.

I am appreciative of Jelle Sleeboom for sharing his expertise on the MDA MB 231 cells and his advice on microfluidic design.

I would like to thank Michelle Vis, for sharing her tips and tricks about microfluidic setups and her interest in my work.

Thnaks to Jaap de Hullu, for his excellent pragmatic suggestions and solutions, and for his ever jovial attitude in the lab.

I thank Arthur de Jong, for helping me with my never ending questions about the microscopes and for helping me look critically at my experiments.

I Would like to thank all the people in the MBx and Microsystems groups who assisted me during my project. The overwhelming help and support I received from so many people made my graduation project such a good experience. The amount of help I received was so considerable that I am undoubtedly forgetting some names. If you do not see your name above and if I ever asked you a question or we ever spoke, know I am grateful to you.

Contents

1 Introduction

Cells are exceptionally talkative and are in communication with each other at all times, both in our bodies and in in-vitro culture. All this information is contained in the secretome, the collection of all proteins expressed in the extracellular space. Characterizing and understanding the secretome is a key aspect in understanding cellular behavior[6]. For instance, the secretome can give an indication of the local state of health or infection. Techniques to precisely measure protein expression are therefore crucial for monitoring cell responses upon stimulation.

In the last decades advances in the field of microfluidics have led to the integration of cell culture in microfluidic devices, even resulting in representative in-vitro models of (patho-)physiological mini-tissues, called "organ-on-a-chip" which are used to study these biological processes. Nevertheless, the integration of biosensors on-chip is still in its beginning stages with only 13% of published research in 2019 in the field of microfluidics and organ-on-a-chip containing a biosensor.[2] However, the addition of on-chip biosensors can greatly improve the functionality and impact of these devices [3]. The added value of on-chip biosensing could critically support applications of organ-on-a-chip and help to replace and improve upon animal models and traditional cell culture for drug screening or disease modelling. Additionally, integrated biosensing in microfluidic cell devices can open the way to personalized medicine, where personalized models of patients can be made to diagnose and screen treatment options.

Consequently, physiologically relevant models with integrated biosensors are promising to both medical research and healthcare. In cancer research for instance, cell metabolism can provide information about tumor development and can therefore be used to screen drugs. These considerations lead to the goal of this graduation project, formulated at the end of this section. This project is a first step in the direction of a device that integrates both a cell culture and a biosensor to examine the response of breast cancer cells upon stimulation. In the future, continuous biosensing such as Brownian Particle Motion (BPM) sensors [7] could further improve the functionality of the device.

In the next chapters, the background of this project will first be laid out, including an explanation of the characteristics of the cell types MDA MB 231 and MCF 7 that are used in this project and the current advances in the field of microfluidics. Then, all necessary methods and the associated principles will be explained. Finally, the obtained results will be presented and discussed.

1.1 Research goal

This project aims to develop a microfluidic device to probe the production of interleukin-6 (IL-6), a response upon stimulation of triple negative breast cancer cells, modelled by MDA MB 231 cells. Triple negative breast cancer is an aggressive and treatment resistant type of cancer with a poor prognosis [8]. This type of cancer can metastasize quickly and the risk of metastasis is increased by an inflamed tumor environment [9]. Therefore, the device will probe the response of triple negative breast cancer cells upon stimulation with TNF-α, a cytokine that takes part in the inflammatory response, with the use of an integrated biosensor.

2 Project background and State of the art

This chapter describes the initial steps to conceptualizing a microfluidic device to measure the production of IL-6 by MDA MB 231 cells. First, it lists an inventory of necessary subcomponents. Then, it succinctly presents the background and current state of the art in microfluidic cell culture and provides context for this project. This context is followed by a description of principles that are necessary to understand the techniques used within this project.

2.1 Plan of approach for a microfluidic device with cell culture and biosensor

The first step in this project is to make an inventory of the essential components of a microfluidic device to be able to reach the goal of realizing a chip with a cell culture monitored by a biosensor. These components give an overview of the required approach and what a finalized chip might look like:

- **Cells:** A cell culture is at the center of this project, along with the biomarker of interest produced by these cells. In this project the MDA MB 231 and MCF 7 cell lines are used, and the biomarker that is targeted is the IL-6 cytokine. More details about these cells are given further in this section. The IL-6 production of the cells will be measured in typical conditions in a well plate first. Eventually, IL-6 production will be measured in the microfluidic device.

- **Chamber that hosts cells:** If a cell culture is to be integrated, an environment in which these cells can reside must be integrated in the device. The chosen cell type is adherent and thus the design must take into account that the cells will attach themselves to the surface and cannot be removed or displaced after incubation. The suitability of this chamber can be evaluated by measuring the cell viability inside the device.

- **Biosensor:** A biosensor is a device to measure the concentration of a (bio)chemical target molecule such as a protein into a measurable signal. In this case a biosensor with a sensitivity in the picomolar range is needed. Since sandwich assays are typically sensitive and specific, this is the chosen method to detect such low concentrations in the complex matrix of cell medium. [10] [11]

- **Chamber that hosts the biosensor:** As with the cell culture, there must be a dedicated area for the biosensor in the chip.

- **A system that can transduce the biosensor response into a signal:** After capturing and binding to the protein of interest, one must be able to measure a signal to determine the concentration. In this project, this is done with the help of a microscopy setup imaging a fluorescent light signal. This is made possible by the material of the chip being transparent. The limit of detection of the biosensor and the detection method should be evaluated for this application.

- **Valve:** A valve is needed to separate the cell culture chamber and the sensing chamber. The valve prevents contamination when it is closed and when it is time to sample and analyze the sample it can open. The transport of the sample from the cell chamber

to the biosensor can be realized by opening the valve and flowing the sample in using standard microfluidic equipment such as syringe pumps. The mechanical performance of the valve is to be tested for different flow rates.

2.2 Cell culture

Cell culture emerged at the turn of the last century, when it was first applied using animal cell lines. In the second half of the century the first human cell line, HeLa, originated. Cell culture has since proven to be an invaluable technology in biological research. Today, cell culture is used for many different applications including: developing and producing vaccines, the production of complex proteins, as well as being the basis for tissue engineering and fundamental research of cell processes. [12]

Over the last decades, improvements have been made with respect to prevention of contamination, cell medium contents, and materials for cell culture vessels, but the basic principles of cell culture have remained largely unchanged [1]. The cells are immersed in cell medium containing amino acids, vitamins, inorganic salts, and glucose and are kept in an incubator at 37^oC, 95% humidity and 5% CO_2. Cells are regularly passaged or subcultured, which involves moving a small amount of cells to a new vessel with fresh cell medium. This is done to extend the life of the cell culture by avoiding the senescence caused by high and prolonged cell density. The number of times this process is performed is called the passage count. Cell cultures with high passage counts can show abnormal behavior, and thus keeping this count low is important in generating reliable results.

2.2.1 Breast cancer cell lines

The cell lines chosen in this project have to meet a few criteria. They should produce a biomarker in response to a stimulus, be of clinical interest and relevance, be robust in order to successfully maintain them, and finally they should to be a suitable candidate for integration in a microfluidic chip.

Following these criteria the breast cancer cell lines MDA MB 231 and MCF 7 were chosen for this project. Both are well-established lines to study breast cancer biology. MCF 7 is a cell line that is primarily used in the development of chemotherapeutic drugs and research into drug resistance.[13] MDA MB 231 is a triple negative breast cancer cell line. This aggressive form of cancer has limited treatment possibilities. Thus the MDA MB 231 cell line is a crucial cell type for developing effective drugs and therapies. This line is also a proven model for breast cancer metastasis, particularly to bone. Metastatic cancer is associated with higher morbidity and mortality making it an essential mechanism to study and understand.[14] Additionally both of these cell lines are adherent, robust and easily cultured, as well as having been proven to be able to be cultured in a microfluidic device in previous research.[15]

The specific biological process that will be observed using these cells is the production of the IL-6 (interleukin-6) cytokine over a few hours as a result of TNF-α (Tumor Necrosis Factor alpha) stimulation. IL-6 has been reported to play crucial a role in metastasis and the progression of cancer in general.[5] Pro-inflammatory cytokines such as TNF-α and IL-6 contribute to a chronically inflamed tumor micro environment which leads to an increased

risk of metastasis.[9] Studying this mechanism is thus important to understand cancer progression and developing potential treatments. However, the connection between high levels of IL-6 and cell migration or invasion are not yet understood in triple negative breast cancer, here represented by the MDA MB 231 cell line. [16] Additionally, a crucial difference between the MCF 7 and MDA MB 231 cell lines is their production of IL-6. The MDA MB 231 cell line secretes IL-6 while the MCF 7 does not secrete IL-6 both with and without TNF-α stimulation. [9] As the goal of this project is to monitor IL-6 concentration the MCF 7 cells are a suitable candidate for control experiments to observe the blank response of a biosensor with a similarly complex matrix.

Moreover, beyond the connection between IL-6 concentrations and breast cancer metastasis, IL-6 is an interesting marker to target as many other pathologies present higher levels of IL-6 in the body. Examples include; post-transplant lymphoproliferative disease with IL-6 levels rising to 11020 pg/mL, and sepsis with concentrations reaching 100000 pg/mL.[17]

2.3 Microfluidic cell culture

As described above, traditional cell culture has not changed much in the last decades. However, more accurate and controllable methods are needed for deeper analysis of cellular processes ranging from single cell analysis to bulk responses in cultures that imitate physiology. Cellular biochemical parameters and signaling are continually changing, which makes a dynamic analysis of cells and their responses crucial to comprehend biological processes.[1] Microfluidic cell culture offers a solution to these demands.

Microfluidic cell culture involves the use of microfluidic techniques, the manipulation of small volumes of fluid, to grow and maintain a cell culture in a chip.[18] Studying chemistry and biology using microfluidics has many advantages such as faster response times, for sensor results for instance, low reagent volumes and the potential for further integration. In cell culture, the most crucial aspect is the ability to completely tailor the cellular micro-environment. Microfluidic cell culture enables new possibilities such as; the possibility to rapidly and dynamically control temperature, to stimulate and analyze simultaneously, to automate experiments, to perform experiments with many different conditions in parallel, and to control nutrients precisely. This technology permits considerable control over soluble factors, temporal and spatial gradients and patterns that cannot be achieved within traditional cell culture methods in flasks or well plates.[19]. Typical examples include the control of glucose [20] and oxygen concentration [15][21] by creating precise concentration gradients or timed concentration variations. This ability to design the cellular micro-environment extends to the possibility to accurately control stimulation concentrations, such as that of TNF-α.

The needs of cells remain the same but are met differently in microfluidic systems than in traditional methods. The oxygen needs can be met by simply making use of the high diffusivity of oxygen in PDMS (Polydimethylsiloxane), which microfluidic chips are often made of. Nutrients and adequate pH are commonly delivered through medium flown through the chip. The remaining factor to consider is the temperature. The temperature is generally controlled off-chip by placing the whole system in an incubator. In some instances it can also be done on chip; some examples will be discussed in section 2.3.3.

2.3.1 Organ-on-a-chip

Beyond traditional 2D microfluidic cell culture, in the last decade efforts have been made to create physiologically relevant models on chips. This field, called organ-on-a-chip, aims at reproducing 3D cellular structure faithfully mimicking (parts of) human organs in microfluidic devices. These models are interesting because they can improve upon the physiological relevance of traditional (2D and static) cell culture and animal models.[22] [23] Traditional 2D cell culture in flasks and wells, while it can give some information on compound efficacy and toxicology, cannot accurately model physiology and cell functions. Animal models, on the other hand, are sometimes a poor representation because animal and human biology simply differ. Additionally, the use of animal models raises ethical concerns.

Organ-on-a-chip could replace these current standard methods in research and, in the future, in drug development and diagnostics. A miniaturized analogue of a human organ could be used in the same fields, of drug testing, and disease modelling, and surpass the performance of both traditional cell culture and animal models.[23] Furthermore, organ-on-a-chip and other microfluidic cell culture technologies could be applied to realize personalized medicine. In this application the aim is to create an in-vitro model that closely resembles the physiology of a specific, individual patient. This could, for instance, be used to screen for the optimal personalized treatment. [24]

2.3.2 Integration of biosensors with cell culture on a chip

The integration of biosensors is a promising emerging trend in microfluidic cell culture and organ-on-a-chip devices. Of the papers published in the field of microfluidics and organ-on-a-chip in 2019, only 13% included a biosensor [2]. Only a limited amount of biosensors have been integrated so far, even though different sensor principles, such as electrochemical, acoustic, and optical, have already been developed [25]. However, on-chip sensing can greatly improve the functionality and impact of cells or organ-on-a-chip devices. The integration of sensing can contribute to making the next generation of physiology models more accurate, reliable and scalable, as well as increasing the speed of analysis [3]. In cancer research specifically, information about the cell metabolism can elucidate tumor development and can be used to test the efficacy of drugs.

2.3.3 Selected examples of microfluidic devices sensing cell secretome

This section discusses a selection of microfluidic devices with an integrated sensor and cell culture presented in literature. These devices are shown in Table 2.1, Figures 2.1, 2.2, and 2.3 and differ greatly. The different design choices will be examined in the light of the goals of this project.

The devices presented in Figures 2.1, 2.2, and 2.3 all measure the concentration of a protein secreted by cells. Device A measures the concentration of IL-2, a cytokine, produced by murine lymphoma cells, which are a type of cancer. Device B looks at the producted HGF and TCF-β1, also cytokines, by hepatocytes (liver cells). And Device C senses the concentration of insulin, produced by islets of Langerhans (pancreas cells).

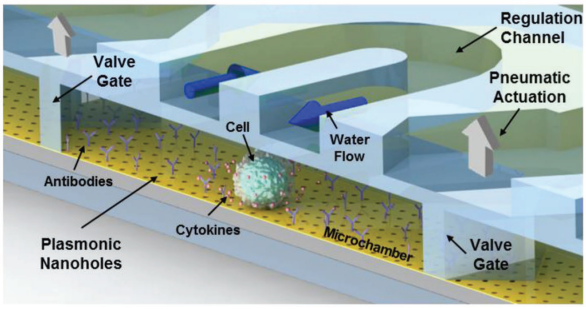

Figure 2.1: Device A: Microfluidic device hosting lymphoma cells using a plasmonic nanohole array to measure IL-2 concentration [26]

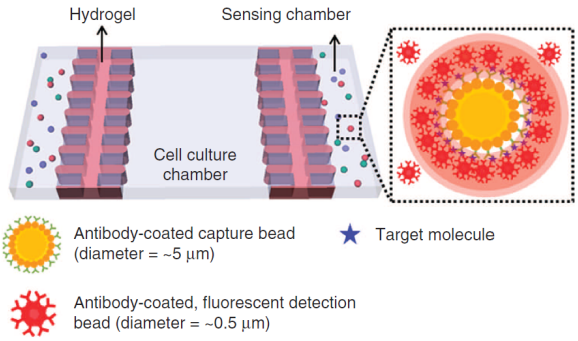

Figure 2.2: Device B: Microfluidic device hosting hepatocytes using a microbeads assay to measure HGF and TCF-β1 concentrations [27]

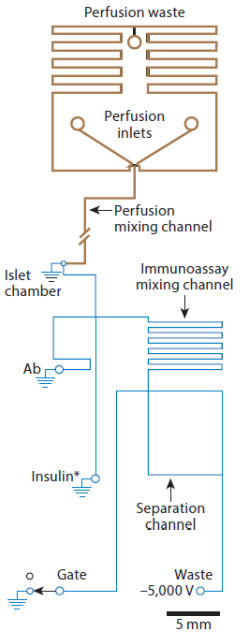

Figure 2.3: Device C: Microfluidic device hosting islets of Langerhans using a competition assay to measure insulin concentration [6]

	Device A	Device B	Device C
Cell type	EL4 murine lymphoma cells	Primary rat hepatocytes	Islets of Langerhans
Analyte	IL-2 (cytokine)	HGF and TCF-β1 (cytokine)	Insulin
Concentration range	3-70 pM	50-200 pM	12-70 μM
Detection method	Immunoassay on plasmonic detector	Sandwich immunoassay with beads	Competion immunoassay with fluorescence
Duration of experiment	Minutes to hours	Several days	Minutes to hours
Heat source	Warm water channel	Incubator	Resistive, thin film

Table 2.1: Three examples from literature of device characteristics of various microfluidic devices integrating both a cell culture and a biosensor

As can be seen in Table 2.1, these devices host different cell types. The lymphoma cells from device A only produce IL-2 upon stimulation. This is similar to the type of behavior that is expected within this project. The stimulating protein is included in the medium prior to analysis. But, the MDA MS 231 and MCF 7 cells used in this project differ from these lymphoma cells in that they are not cultured in suspension. A suspended cell line enables the method of simply flowing in the cells and performing analysis immediately, as presented in device A. In device C, the cells are also in suspension and simply pipetted in a open chamber prior to measurement. However, the cell type used in this project is adherent and thus, a first incubation time is needed to enable the attachment of cells to the device. This is similar to the hepatocytes of device B, which are first incubated overnight to allow the cells to attach to the microfluidic device. This affects the design of the chip, since a barrier and sampling mechanism are needed to prevent the cells from attaching in the sampling region overnight. Thus, a similar approach can be taken for the design and experiments with the breast cancer cells.

The detection methods and assay types are different across all three devices shown in Figures 2.1-2.3. In both device A and B, the target of interest is a cytokine. In Device A, since plasmonic detection is particularly sensitive in changes to the surface of the detector, only using a capture antibody suffices. In device B, however, a sandwich immunoassay is used. Sandwich immunoassays are typically very sensitive, specific and robust.[11] They are therefore a good choice for the low concentration ranges observed here. Device C employs a competition assay and targets a much higher analyte concentration. Competition assays are typically less sensitive than sandwich assays. As such, competition assays are typically only used for small targets were there is no possibility to use antibody pairs. [10] [11] Consequently, in this project, a sandwich assay is the best choice to determine the concentration of a cytokine in the pM range, in a complex matrix.

As is clear from Table 2.1, the durations of the different experiments vary greatly; from a few minutes to a few days. This difference in experimental design requires a different choice of heating source in the chip design. Both Device A and C have shorter running experiments where a heat source is integrated into the chip. However, as discussed above, the device with adherent cells is incubated overnight which increases the duration of the use of the device in the experiment. Additionally, the IL-6 production will be measured over a few hours. This makes on chip heating much less advantageous compared to simply putting the whole device into a cell incubator. Thus, this method seems most suitable to the specific needs of this

project.

2.4 Background needed for the project

This section introduces and explains several principles that are necessary in understanding the work and design choices made in this project. Due to the multidisciplinary nature of this project, this section also explains some common, yet field specific, concepts.

2.4.1 Biosensor and sensitivity

A biosensor is a device to measure the concentration of a (bio)chemicaltarget molecule such as a protein into a measurable signal. The definition of a biosensor is very broad, thus, in the interest of brevity, only principles of importance for this project will be treated.

An essential component of a biosensor is typically a binding molecule to target the specific biomarker of interest. The biomarker in this project, IL-6, is a protein, which is commonly captured using antibodies. However, also other capture molecules such as aptamers exist. After binding, a mechanism is needed to translate this capture into a signal. This signal can be a multitude of different things including a light signal, an electrical signal, or other. However, every signal suffers from noise. The limit of detection (LOD) is the lowest analyte concentration at which the corresponding signal can be clearly discerned from this noise[28]. It is defined mathematically as:

$$S_{LOD} = S_b + 3\sigma_b \tag{2.1}$$

where S_{LOD} is the signal at the limit of detection, S_b is the signal at blank and $3\sigma_b$ is the standard deviation of this signal at blank. In the case of a linear relation between the signal and the concentration the LOD becomes:

$$S = c \cdot a + S_b \tag{2.2}$$

where c is the concentration of the analyte, a is the slope of the linear relation and where the intercept is equivalent to the signal at blank S_b.

$$LOD = \frac{(S_b + 3\sigma_b) - S_b}{a} = \frac{3\sigma_b}{a} \tag{2.3}$$

Beyond the LOD, which only guaranties a readable signal above noise, there is the limit of quantification (LOQ). Above the LOQ, two different signals caused by different concentrations can be reasonably discerned. The LOQ is defined in a similar manner as the LOD.

$$S_{LOQ} = S_b + 10\sigma_b \tag{2.4}$$

In the case of a linear relation,

$$LOQ = \frac{(S_b + 10\sigma_b) - S_b}{a} = \frac{10\sigma_b}{a} \tag{2.5}$$

2.4.2 Fluorescence

Fluorescence is an often-used property in biosensors and microscopy techniques. This form of luminescence is the emission of light by a substance after absorbing incident light (electromagnetic radiation). The phenomenon occurs when an excited molecule, or material relaxes from a high energy state to a lower one. A Jablonski diagram, as pictured in Figure 2.4, depicts these transitions between energy levels. The material is first struck by an incident photon, which excites the dye molecule to a higher electronic and vibrational level. First, the system relaxes vibrationally. Afterwards, the system fluoresces by transitioning down to the lower electronic energy level. As can also be understood from Figure 2.4, the emitted light has a lower energy, or longer wavelength, than the exciting light. This difference is called the Stokes shift. A good example to illustrate this shift is the dye Alexa Fluor 568, used in this project,which has a excitation wavelength of approximately 578 nm (orange) and an emission wavelength of 603 nm (red).

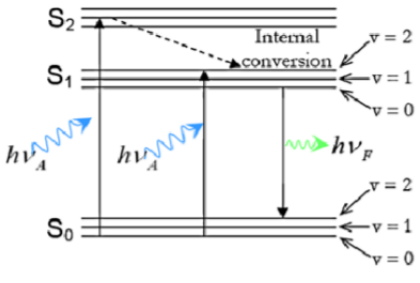

Figure 2.4: Schematic Jablonski diagram depicting the energy transitions leading to fluorescence [29]

2.4.3 Flow characteristics in microfluidics

The flow in a microfluidic chip is different from typical macroscopic flow behavior in that, by its scale, it is dominated by viscous effects. The flow inside a microfluidc chip is therefore typically laminar. In addition, surface tension has a much greater effect than in macroscopic fluid flow.

Reynolds number The Reynolds number is a dimensionless number that can be used to asses whether flow can become turbulent or remains laminar. It weights the ratio between of inertial forces against the viscous forces in the flow, as can be understood from equation 2.6.

$$Re = \frac{\rho u L}{\mu} = \frac{\rho u D_h}{\mu} = \frac{\rho u}{\mu} \frac{2wh}{w+h} \tag{2.6}$$

Where Re is the Reynolds number, ρ the density of the liquid in kg.m^{-3}, u the flow speed in m.s^{-1},μ the dynamic viscosity in Pa.s, and L is the characteristic dimension in m. In flow through a channel, the characteristic dimension can be defined as the hydraulic diameter D_h, which in the case of a rectangular channel is : $2wh/(w+h)$, with w the width of the rectangle and h the height.
In the case of a high Reynold number, the flow is an inertia dominated flow, which can develop into turbulence, involving vortices and chaotic flow instabilities. This is what one

can typically experience in macroscopic flows. In the case of a low Reynolds number, as it often is in microfluidic devices, the flow is dominated by viscous forces and characterized by a smooth flow, and the flow is laminar.

Fluidic resistance In channels, including microfluidic channels, there is a resistance to flow called flow resistance. In the microfluidic device, as discussed, the Reynold number is low which indicates a behaviour dominated by viscous effects. In the case of a laminar flow through a rectangular channel such as the ones in the presented device the resitance is defined as [30]:

$$R = \frac{1}{1 - 0.63(h/w)} \frac{12\mu l}{h^3 w} \tag{2.7}$$

Where R is the fluidic resistance in Pa.s.m^{-3}, l the length of the channel in m, h the height of the channel in m, w the width of the channel in m. One can see from equation 2.7 that in the case of a narrower channel, a smaller w, the resistance will increase. This property can be used to increase the flow in certain directions, by increasing the resistance in areas where one wants to prevent undesired flow.

Capillary pressure Surface tension (or interfacial tension) can be used to describe the tendency of liquids to minimize their exposed surface area. This is caused by the cohesive forces of the molecules at the air-liquid surface being pulled towards the rest of the liquid.

Wetting is used to describe the interaction of a liquid with a surface. It is characterized by the contact angle of the liquid with the surface. With water, in case of a contact angle of more than 90°the surface is called hydrophobic and the surface is called hydrophilic for contact angles smaller than 90°.

Capillary pressure occurs as a result of the combined effects of surface tension and wetting of the walls of a narrow channel. An example of an effect caused by capillary pressure is the advancement of water inside a (hydrophilic) glass capillary. The capillary pressure is defined as the difference between the pressure inside (P_i) and outside (P_o) of the liquid, and is calculated using [31]:

$$P_i - P_o = \Delta P_c = -\sigma(\frac{1}{R_1} + \frac{1}{R_2}). \tag{2.8}$$

Were σ is the surface tension, and R_1 and R_2 are the principle radii of curvature, as pictured in Figure 2.5.

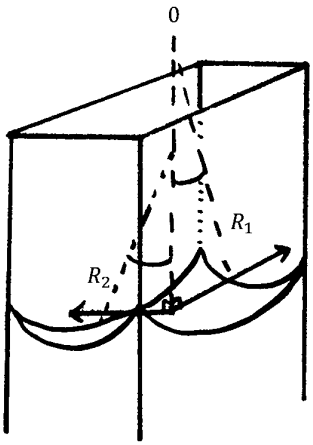

Figure 2.5: Diagram depicting the surface of a liquid in a capillary. R_1 and R_2, the principle radii of curvature are indicated.

For a symmetrical capillary:

$$\Delta P_c = -2\sigma \frac{1}{R} = -\frac{2\sigma cos\theta}{r} \tag{2.9}$$

Were the radius R can be calculated using the contact angle θ between the wall and the liquid and the diameter of the capillary $R = \frac{r}{cos\theta}$. In the case of a rectangular channel [32]:

$$\Delta P_c = -2\sigma(\frac{cos\theta_w}{w} + \frac{cos\theta_h}{h}) \tag{2.10}$$

Were w is the width and h the height of the channel. As one can see the pressure is either positive or negative depending on the contact angle as a result of the surface inside the capillary. This pressure can pull liquid in the narrow channel or create a pressure barrier that pushes the liquid out. This effect only plays a role in the case of a partially filled microfluidic device. Once a chip is completely filled with water, the air-liquid interface is not present inside the chip anymore.

3 Methods

This section describes the most important techniques and methods used in during this project. More precise protocols can be found in the appendices of this report.

3.1 Biosensor techniques

In the experiments of this project the aim is to quantify the IL-6 prodution MDA MB 231 and MCF 7 cells when stimulated using TNF-α. In both well plates and microfluidic devices, the cells are counted, seeded and then incubated overnight and stimulated with cell medium containing TNF-alpha the next day, or left unstimulated. Next, quantification methods are needed to determine the concentration of the produced IL-6.

3.1.1 Sandwich assays

An often used technique in the experiments of this project is the ELISA or Enzyme-Linked ImmunoSorbent Assay. Like all sandwich assays this is a sensitive and specific [11] technique to measure the concentration of a ligand, which is often a protein, in this project is the IL-6 protein.

Sandwich ELISA A sandwich ELISA is performed in several steps as pictured in Figures 3.1a to 3.1e. These steps are performed in micro wells, which are thoroughly washed after each step to clear out the remaining reagents. First, a surface is coated in excess capture antibodies. Then the sample, taken from the cell culture in a well or chip, with the protein of interest is introduced and the protein binds to the capture antibodies. Next a biotin-detection antibody conjugate is bound to the captured antigen. A streptavidin-HRP conjugate is then added and binds with the biotin from the previous step. TMB (Tetramethylbenzidine) substrate is subsequently added, which by reacting with the HRP creates a blue colored product in proportion with the concentration of the captured antigen. To stop the reaction an acid is added and the results can then be read by measuring the absorbance at a specific wavelength. A curve is fitted using known standard concentrations, and the concentration in the samples can then be calculated using this fit.
Because this protocol relies on absorbance, which is proportional to path length, it is well suited to well plates. The reagents in the wells have a thickness of approximately 5mm. However, the microfluidic device has a height in the range of 100μm.

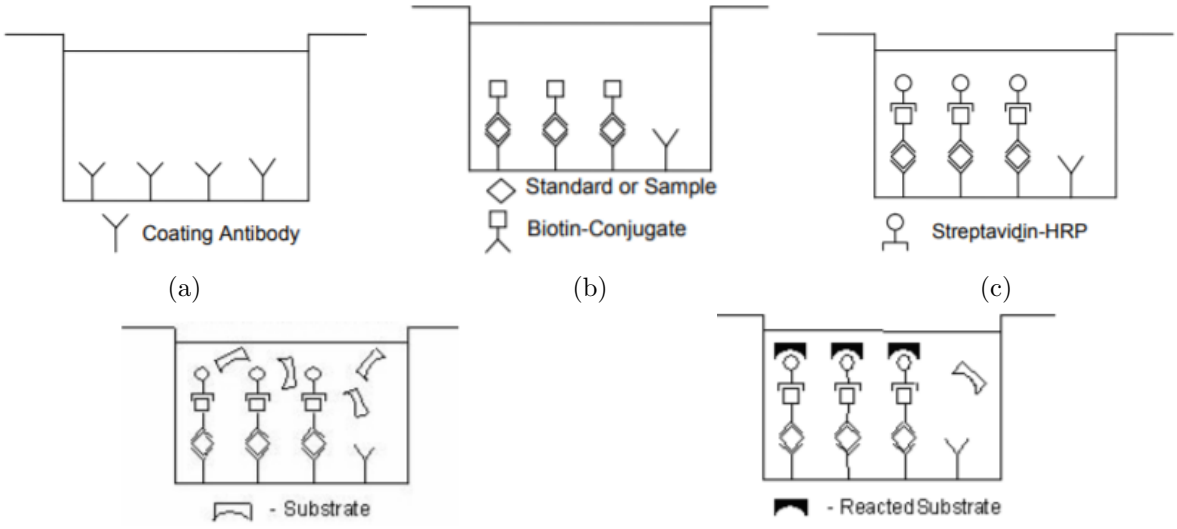

(a) (b) (c) (d) (e)

Figure 3.1: Protocol for ELISA: (a) The microwell is coated in capture antibody (b) Samples and standards as well as Biotin conjugate is added to the wells (c) Incubate with streptavidin-HRP, which binds to Biotin (d) Incubate with TMB substrate until sufficient colored product has formed (e) The reaction is terminated by the addition of acid and results can be read [33] [34]

Fluorescent sandwich assay Since an ELISA would not be suited inside a chip because of the limited height, a different method is needed. A technique that is not depended on chamber volume is the simple sandwich immunofluorescence assays (sIFA). This method is akin to the ELISA technique described previously in that it is both selective and sensitive by implementing the use of two antibodies, a capture and detection antibody, as pictured in Figure 3.2. The detection antibody is connected to a the fluorophore, which can be done in a number of ways, in this project a biotin-streptavidin connection was used. Alexa Fluor 568, a red-orange dye, was chosen as a marker to avoid the green auto-fluorescence of the breast cancer cells. In this technique the concentration of the analyte is proportional to the number of fluorophores present after washing. This light signal is then captured to be able to determine the concentration of analyte in the sample.

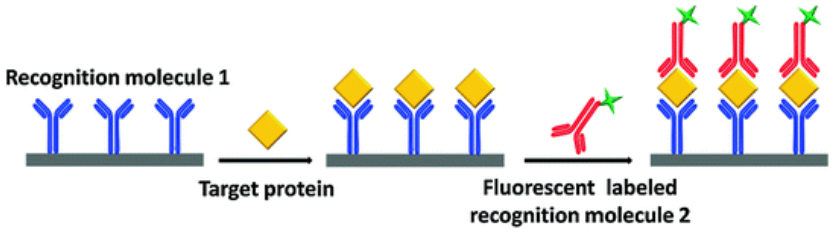

Figure 3.2: Schematic representation of a fluorescent sandwich assay[35]

Viability assay Another use of fluorescence is the cell viability test performed within this work. This assay is performed to evaluate the suitability of the microfluidic device to host a cell culture. The cells are seeded and incubated overnight in the same manner as the other

experiments, and a viability assay is executed on the cell culture inside the chip. The viability assay consists of two different dyes, one that fluoresces blue that is able to stain all cell nuclei and a red one that stains only the nuclei of cells with compromised plasma membranes. Both of these dyes bind to DNA but the blue dye (NucBlue) is a Heochst dye, which means it can permeate through the cell membranes and stain all cells[36]. The red dye, propidium iodide, only enters the (dead) cells with damaged membrane and its fluorescence is increased 20 to 30 times once bond[37]. Thus, making very bright spots at the locations of dead cells. After staining the cells using these two dyes, an image is captured of the cells with two filters. Thus, using two different filters one can examine two different pieces of information on the same sample. The proportion of dead and live cells can then be calculated. Generally speaking a cell viability, the proportion of live cells, above 80% is considered good[38], [39], [40]. An example of the resulting images can be seen in section 4.2.

Once these images are obtained, the are analyzed using an image analysis software (ImageJ) to count the live and dead cells. A threshold is placed on the image to separate the dark background from the bright cells and a particle counter counts the number of cells.

3.1.2 Fluorescent microscopy

Filters for fluorescent microscopy The Stokes shift, as described in section 2, of the dyes used in this project can be exploited to separate the incident light and the emitted fluorescence by using a filter. The filters used, pictured in Figure 3.3, separate the bright background from the produced fluorescence and thus create an advantageous signal to noise ratio. The filter cube used in this project contains a combination of a bandpass filter to allow the correct range of light for excitation. A dichroic mirror reflects the excitation light onto the sample and lets the emitted light pass to the ocular upon return. Finally, a filter at the emission wavelength lets the fluorescent light pass to the objective.

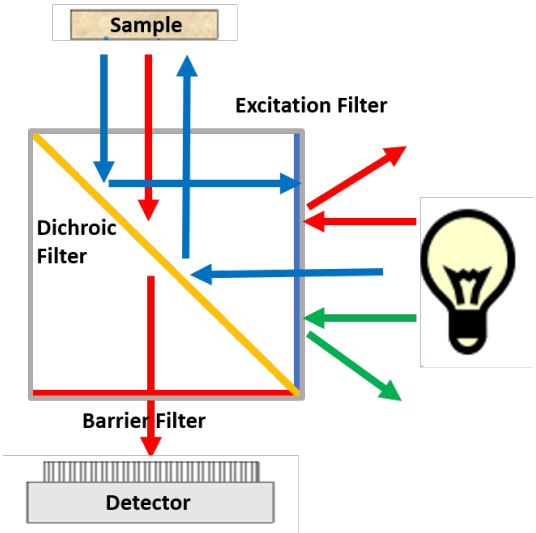

Figure 3.3: Schematic diagram depicting depicting a filter cube used in fluorescent microscopy [41]

Alexa Fluor 568, which was used in determining the sensitivity of the biosensor setup, has an

excitation peak at 578nm and an emission peak at 603nm. The suited filter cube has a first bandpass filter at 580/20nm (centered at 580nm and FWHM of 20nm) a dichroic mirror with a cutoff at 595nm and a second bandpass filter at 630/55nm. NucBlue, used in the viability assay has an excitation peak at 360nm and an emission peak at 460nm. The filter chosen for this dye has a first band pass filter at 360/40nm, a dichroic mirror at 400nm and a second filter with a longpass at 425nm. Propidium iodide, also used in the in the viability assay, when bound, has an excitation peak at 535nm and an emission peak at 617nm. The filter that suits this dye has a first band pass filter at 545/40nm, a dichroic mirror at 565nm and a second filter with a bandpass 610/75nm.

Quantifying a fluorescent signal The resulting light signal cannot simply be translated to a concentration without additional information. First samples of known standard concentrations are prepared, and the resulting image is captured by using a microscope with the correct fluorescent filter and a camera. Fluorophore-streptavidin (Alexa Fluor 568) conjugates were physisorbed onto a glass surface. The excess was then washed away which creates a monolayer of fluorophores to approximate the fluorescent signal coming from a sIFA. The light from the fluorophores is captured using a wide-field epifluorescent microscope with a camera. Different objectives, with different numerical aperture (NA), are used in order to optimize the captured images. After capturing the first image, care is taken to keep the gain, gamma and brightness settings the same, only the shutter time and frame rate are altered to attempt to capture a brighter image.
The average brightness from these images is computed by using a MATLAB script, with completely black pixels having a value of 0 and completely white ones a value of 255. Thus, a standard curve to connect the brightness and concentration can be created. From this curve the LOD and LOQ of the fluorophores can be determined, using the formulas described in section 2.

3.2 Microfluidic chips

3.2.1 Fabrication techniques

Design The first step to creating the design are evaluating all the requirements preferences and constraints that the design of the microfluidic device should adhere to. A few components have already been identified in section 2.

- The design should have a cell culture chamber capable of hosting an adherent cell culture. The correct temperature humidity and gas composition is ensured by placing the device in an incubator. Furthermore, the cell chamber should be larger than the biosensor chamber to make sure that the sample volume is sufficient to fill the biosensor chamber and the channel leading up to it. The cell chamber should also feature a central column to prevent the chamber from collapsing from manipulation of the PDMS device during fabrication.

- The design requires a sensor chamber. The minimum dimensions of the biosensor chamber are determined by the field of view of the microscope, and, as stated, should be smaller than the sample volume in the cell culture chamber.

- A valve is required to separate the cell culture chamber and the sensing chamber. However, the incubator that the microfluidic device will reside in does not have the equip-

ment necessary for pneumatic or electrical actuation. This places a constraint on the possible actuation methods for the valve. For this reason a screw valve seems the best choice[42] [43]. These valve are entirely self contained on the chip and do not need external actuation equipment besides a simple hex key.

- The design should feature quite wide channels to prevent clogging by the cells, which have a diameter of approximately 20μm, and could be washed away.
- The size of the design is constrained by the size of a microscopic slide.
- The width of the channel is constrained by the size of the bolt used in the valve.
- The size of the inlets and outlets is constrained by the size of the needles and punch tools needed to pierce the PDMS.
- Any changes in width are preferred to have smooth edges to prevent air bubbles being trapped in the device.

Considering these requirements, constraints and preferences, the design for the device is drawn up, and the result is shown in Figure 3.4. This design features overall rounded corners and smooth transitions in channel width. The cell culture chamber is indicated by the letter A in Figure 3.4 and has a volume of 12μL and a central column. In B one can see the biosensor chamber with a volume of 2μL. The screw valve will be located in C. The inlets and outlets are indicated by D and E respectively. F points to the main channel which has a width of 1mm and a height of 130μm to prevent clogging. G indicates the side channel leading to the sensor chamber. The width of this channel is 500μm to ensure for easy placement of a M2,5 bolt for the valve and to limit leaking and assist the valve by way of hydrodynamic resistance.

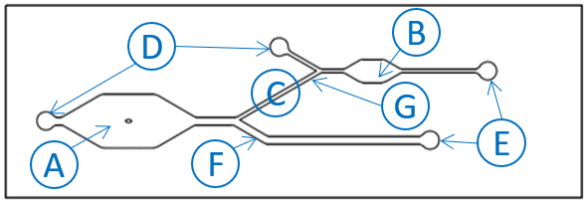

Figure 3.4: Device design made usind AutoCAD software
A: the cell chamber, B: the sensor chamber, C: valve location, D: inlets, E: outlets, F: wide main channel to outlet, G: narrow side channel to the sensor chamber

Photolithography After receiving a photomask according to the chip design, the process to create a mold can begin. The chip mold is made on a silicon wafer using a photolithography process with the negative photoresist SU-8, pictured in Figure 3.5. First, photo-resist is applied to a wafer using a spincoater. The thickness of the photoresist is determined buy the rotational speed and acceleration of the spincoater. To program the adequate spin coating protocol the instructions of the manufacturer of the chosen SU-8 photoresist are followed. The precise protocol use is described in the Appendix in section A. After spin coating, the wafer is baked once before exposure, which is the pre-exposure bake or soft bake. The photomask is then put onto the wafer with photoresist and exposed using UV-light. In this step the exposed SU-8 photoresist's long molecules cross-link and the photoresist thus solidifies.

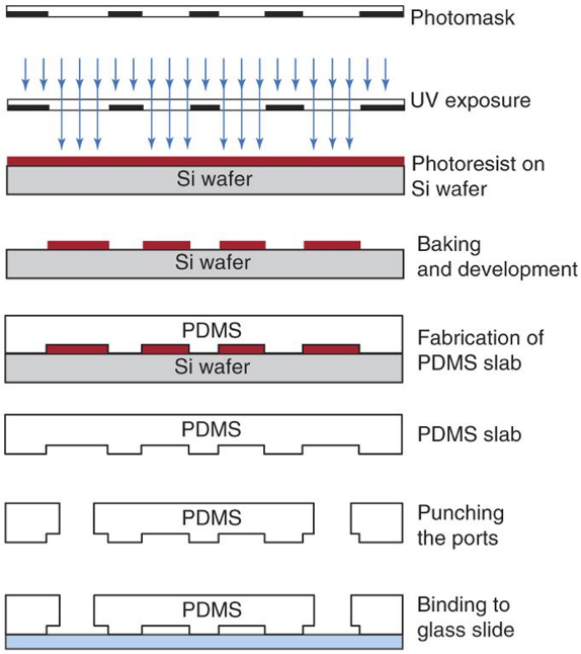

Figure 3.5: Schematic representation of the soft lithography process [44]

During the development step, the remaining unexposed photoresist is washed away, creating a negative image of the photomask, hence the name negative photoresist. After developing, an optional bake, called hard bake, is performed to improve the mechanical properties of the mold by annealing small cracks and stresses and ensuring the behavior of the mold stays consistent when it is exposed to high temperatures at a later stage. After cooling the mold, as shown in Figure 3.6, is now ready to be used.

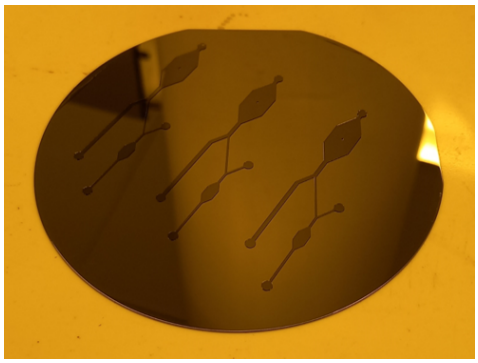

Figure 3.6: Succefully prepared silicon wafer to use as a mold for PDMS devices

PDMS molding To create the microfluidic chip, PDMS is molded on the previously prepared wafer. First the PDMS is prepared by mixing polymer base and a curing agent, resulting in a viscous liquid. This liquid is then poured onto the mold and degassed inside a desiccator to ensure it is free of bubbles before curing in an oven. After curing, PDMS acts as a solid rubber, capable of holding the desired shape of the microfluidic device.

Valve fabrication The valve integrated in the chip is a design that uses a bolt and nut system to pinch a microfluidic channel shut. [42] [43] To create this valve the chip design is first molded in PDMS as described above, however the PDMS is only partially cured in this step. This is to ensure proper adhesion to the next layers. Next the bolt and nut are placed onto the chosen channel in the device. The details of the method are pictures in Figure 3.7. The thread of the bolt should be wider than the channel that will be actuated to ensure easy alignment and proper closure. The bolt and nut are stabilized by using a previously punched ring made out of completely cured PDMS with an inner diameter the size of the thread. Then, a second layer PDMS is poured onto the device, encasing the bottom half of the bolt, making sure the nut is completely submerged. The whole device is then cured and the result is a chip with an embedded bolt and nut that can act as a screw valve and close and open the channel underneath.

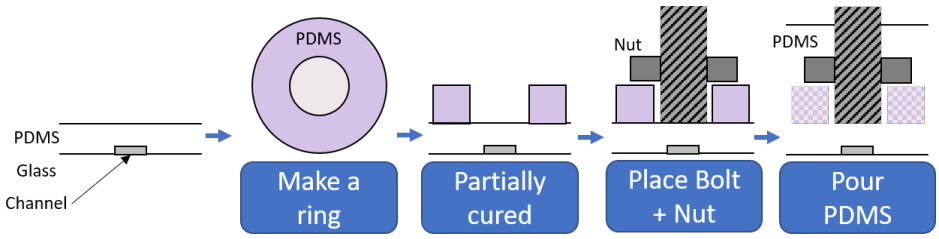

Figure 3.7: Fabrication method to create a bolt-nut valve embedded in PDMS

Finishing the device Finally to finish the device the underside must be closed off. It is peeled away from the mold, cut and bonded to a glass microscopy slide after performing a plasma treatment to the glass and the bottom of the PDMS. When it is time to use the device inlet and outlet channels are punched out using a dermal punch. Then, it is connected to tubing by inserting needles in the outlets and inlets as shown in Figure 4.9. The needles can be autoclaved and can thus be reused after being exposed to bio-hazardous materials such as the ones used in this project.

Mechanical testing After fabrication the mechanical aspects of the finished device should be tested. The performance of the valve in particular is crucial for this design. Testing the valve can be done by using a syringe-pump to flow water at known flow rate through the chip in both open and closed states. The goal is to observe whether the valves fails or leaks, which can be viewed through a microscope. Flow rates ranging from 10μL/min to 5mL/min should be tested in this manner.

4 Results and Discussion

In this section the results of the experiments performed in this project are laid out.
The first step taken in this project is the quantification of the IL-6 produced by the breast cancer cells in order to have a baseline to compare for the following steps with. Then, the performance of the microfluidic device is tested. Both the mechanical performance as well as the cell viability inside the device is evaluated to determine whether the design is suited to the goal of the project. Next, preliminary work on biosensor sensitivity is done to determine whether the sensitivity of the biosensor matches the quantity of IL-6 produced by the cells. Finally, the IL-6 production of cells inside the microfluidic chip is measured and compared to the results obtained in well plates.
For each experiment a goal is laid out. Then, the obtained results are described. Finally, the implications of the results are discussed in light of the project goal and existing literature.

4.1 Quantifying the IL-6 production

The first experiments centered on quantifying the IL-6 production of the MDA MB 231 breast cancer. This information is important for the design of the following experiments inside the microfluidic chip of this project and give a it first indication of the concentration range of interest for the biosensor to be integrated.

First, the effect of TNF-alpha on the cells was observed. An important observation was that upon stimulation, cell migration occurs. To confirm this, an additional experiment, in which cells were stimulated with TNF-α without measuring the resulting IL-6 was performed. The cells were observed by microscope at regular time intervals to examine the reaction to TNF-α. In Figure 4.1 an example of normal and securely attached cells is shown. Figure 4.2, shows cells that were not securely attached and inflamed, and 4.3 shows how the detached cells floated away. As can be seen in Table 4.1, the proportion of loose cells increased both with time and TNF-α concentration. Thus, to avoid practical problems caused by large amounts of loose cells, experiments were only performed with the lower concentration of TNF-α, 10 and 20 ng/mL. However as can be seen further in this section in Figures 4.7, and 4.8, the IL-6 production is not much different with 20ng/mL TNF-α compared to 10ng/mL.

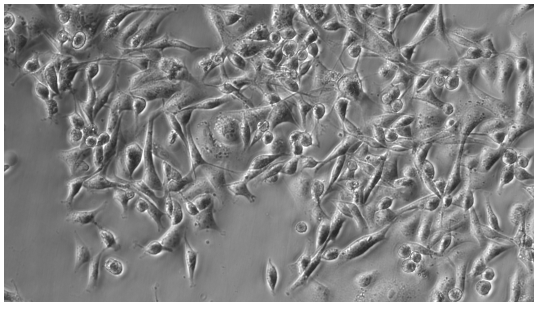

Figure 4.1: MDA MB 231 cells securely attached to the bottom of a well plate

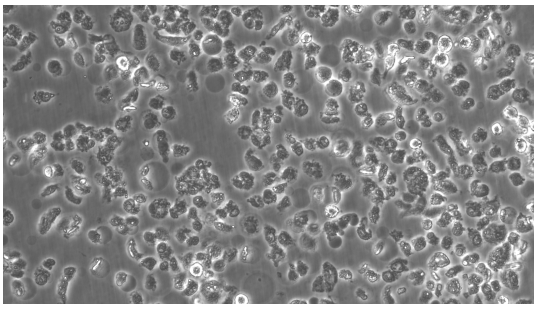

Figure 4.2: MDA MB 231 stimulated using 250 ng/mL cells not securely attached to the bottom of a well plate and seemingly inflamed

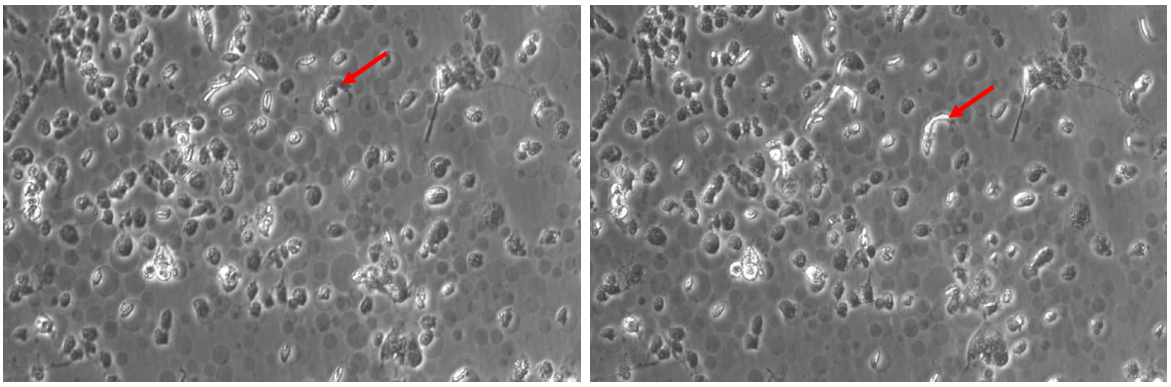

(a) (b)

Figure 4.3: MDA MB 231 cells stimulated using 100 ng/mL TNF-α detached from the bottom of a well plate and floating in the cell medium. For example, the cell marked by the arrow moves between the frames of a video.

TNF-α (ng/mL)	0	10	20	50	100	250
15 min	normal	normal	normal	normal	normal	normal
1 hour	normal	normal	normal	normal	normal	looks irritaed
2 hour	normal	very few detached	normal	few detached	some detached	many detached
3 hour	normal	very few detached	some detached	some detached	quite some detached	many detached
4 hour	normal	very few detached	some detached	some detached	many detached	many detached
5 hour	normal	few detached	some detached	quite some detached	many detached	many detached
6 hour	normal	few detached	some detached	many detached	many detached	many detached

Table 4.1: Observation of the state of cells trough a microscope as a function of TNF-α concentration and time

To determine the IL-6 concentrations produced by the MDA MB 231 and MCF 7 cells an ELISA, as described in section 3.1, was performed on samples taken from cell cultures in a well plate. The cell density was determined upon seeding. More details on the protocol can be found in the appendix in section A. The stimulated cell cultures were incubated using medium that contains TNF-α to promote IL-6 production. Incubation times between 1,5 and 9 hours are observed to complement existing data in literature [9] [5]. This experiment was repeated multiple times and is denoted as experiment 1, 2 and 3 further in this section.

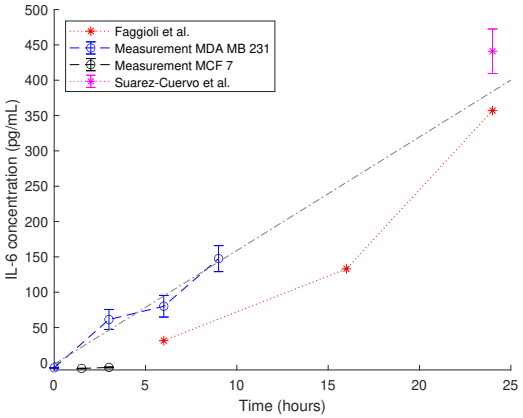

Figure 4.4: IL-6 concentration produced by stimulated (TNF-α 10 ng/mL) cells ($7 \cdot 10^4$cells/mL) as a function of incubation time during experiment 1 compared to literature [9] [5]

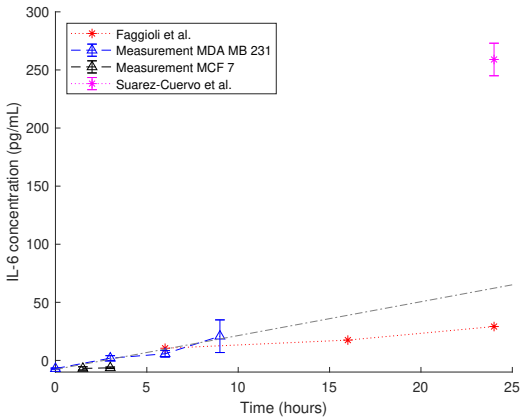

Figure 4.5: IL-6 concentration produced by unstimulated cells $7 \cdot 10^4$cells/mL as a function of incubation time during experiment 1 compared to literature [9] [5]

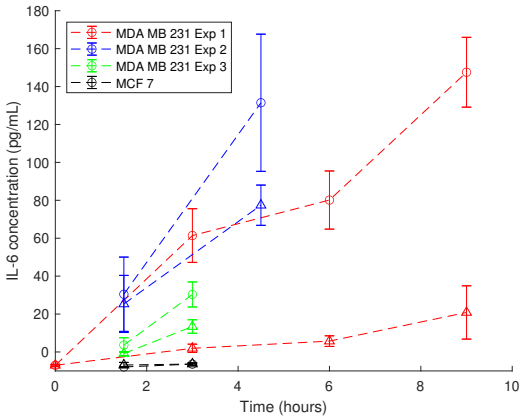

Figure 4.6: IL-6 concentration produced by $7 \cdot 10^4$ cells/mL MDA MB 231 and MCF 7cells as a function of incubation time
The data indicated by a circle are as a result of TNF-α (10 ng/mL) stimulation. The data indicated by a triangle are as a result of basal or unstimulated IL-6 production by the cells. Exp 1, 2, and 3 denote the different repetitions of the experiment. The shown error is a result of the sum of standard deviation in the results over all samples and the precision of the multiwell plate reader according to the manufacturer

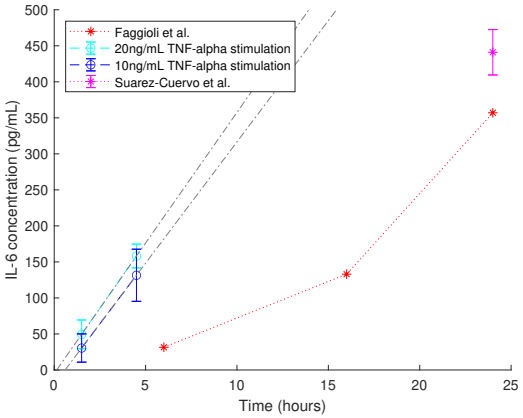

Figure 4.7: IL-6 concentration produced by stimulated (TNF-α 20 ng/mL and 10 ng/mL) MDA MB 231 cells ($7{\cdot}10^4$cells/mL) as a function of incubation time during experiment 2 compared to literature [9] [5]

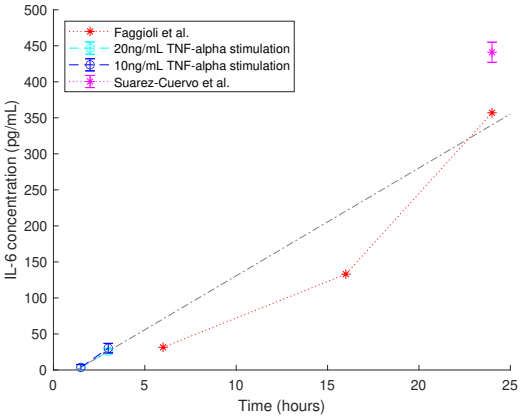

Figure 4.8: IL-6 concentration produced by stimulated (TNF-α 20 ng/mL and 10 ng/mL) MDA MB 231 cells ($7{\cdot}10^4$cells/mL) as a function of incubation time during experiment 3 compared to literature [9] [5]

As can be seen in Figures 4.4, 4.5, 4.8, the IL-6 production rate by the seeded MDA-MB 231 aligns with and complement previous results from literature [9] [5]. The experiment was repeated multiple times for different timescales to have a higher temporal precision. It is of note that upon repetition of the experiments, the resulting concentrations did vary somewhat, as can be seen in Figure 4.6. Overall, the average IL-6 production rate from Figure 4.6 is 2,5 pg/hour/10^4cells for stimulated cells and with 0,7 pg/hour/10^4cells unstimulated cells. This production rate was not altered by a higher concentration of TNF-α, as can be seen in Figure 4.7 and 4.8.

Control experiments were performed using MCF 7 cells, which as mentioned in section 2.2.1 do not produce IL-6. For all instances the MCF 7 cell medium samples yielded a concentration below the ELISA assay range (minimum of 3pg/mL), as pictured in Figures 4.6, 4.4, and 4.5.

Discussion As shown in Figures 4.4 4.5 the obtained concentrations are in line with experiments from literature [9] [5] that were done for longer timescales. These results confirm the seemingly linear increase in IL-6 concentration, and a rate of IL-6 production of around 2,5 pg/hour/10^4cells for stimulated cells and 0,7 pg/hour/10^4cells unstimulated cells. This result is used further in this research to be able to quantify the expected IL-6 production inside the fabricated microfluidic device as a function of cell density and thus gives insight into the desired LOD and LOQ of the integrated biosensor.

As is apparent from the discrepancy in IL-6 concentrations in Figure 4.6 the experiment suffers from reproducability issues. When, the experiment was repeated a a few times as to probe more narrow time intervals, it revealed this difficulty in reproduction. In particular the second time the experiment was performed a large variation was observed between the measurements as well as a difference with the previous results. The standard deviation is the dominating effect on the error, pictured in 4.6. This large variation was likely caused by

inhomogeneous cell seeding leading to a variation in cell count after overnight cell growth. Another possibility is a difference in IL-6 production upon stimulation. This could have been caused by the higher passage count of the cell in the second experiment. Older cells may react differently to the same stimulation. The cells had already been subcultured 68 times by this point. To eliminate this effect, a new cell line was started, and a lower passage count was used in following experiments in the microfluidic chip (passage 55). Upon making sure the cell seeding was particularly homogeneous for the third experiment, a much narrower variation as well as a better accordance with the first experiment was observed.
The reproducability of this experiment can be improved by mitigating these two factors in future experiments both in wells and in microfluidic devices. On the one hand one should use younger cells with lower passage counts to prevent variability in IL-6 expression. On the other hand using more precise cell quantification upon seeding such as automated cell counting and simply making sure the cells are a homogeneous suspension before seeding would improve the heterogeneity between wells.

As MCF 7 produced no detectable IL-6, this cell line is a very good candidate to perform control experiment with a similarly complex matrix. These cells did not produce any detectable IL-6 regardless of stimulation, whereas MDA MB 231 cells did produce some IL-6 even in the unstimulated case. Thus, to perform control experiments where cells and a complex matrix are required, but no IL-6, one can use MCF 7 cells. Complex matrices often cause a large background caused by non-specific interactions. As the IL-6 is only produced by the MDA MB 231 cells at a rate in the pg/hour range, a good protocol is needed to limit these non-specific interactions, which can be developed with the help of the MCF 7 cells.

As discussed earlier in this section, the stimulated cells were observed to detach from the well surface as a result of inflammation caused by the TNF-α stimulation. This seems logical as inflammation is related to a higher chance of metastasis[16]. Furthermore, the IL-6 production does not seem to increase for higher TNF-α concentration. Thus, in following experiments in the microfluidic device, the stimulation will be limited to only 10 ng/mL of TNF-α.
However, there is still some degree of cell detachment for this concentration. This can lead to important practical problems as the cells may move and enter the sensing chamber when the cell medium sample is flowed in. A possible solution to prevent this would be integrating a filter in a future design. The filter should be placed before the biosensor to protect it from damage caused by a cell entering the sensor chamber with the sample. A simple microfilter or membrane could be used [45], although this is susceptible to clogging, or more advanced methods such as deterministic lateral displacement (DLD) [46], or microstuctures such as grooves [47] could be used.

4.2 Testing and validating the chip design

After designing the chip as pictured in Figure 3.4 and fabricating the device by using the methods described in section 3.2, the functions of the resulting device were tested. First, the mechanical properties of the chip pictured in Figure 4.9, and the valve in particular, were tested. Then it was assessed whether the microfluidic environment is adequate to host cells by performing a viability assay as described previously.

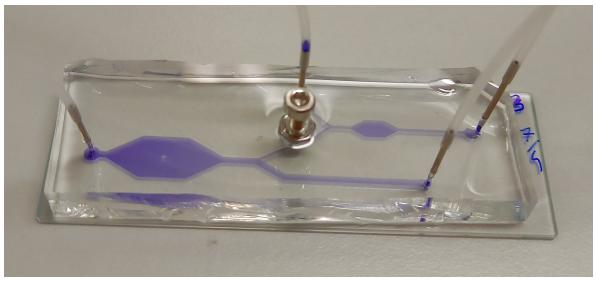

Figure 4.9: Fabricated microfluidic chip with a bolt-nut screw valve filled with ink to make the channels and chambers visible and connected to tubing using needles

4.2.1 Mechanical testing

The valve is the most important mechanical aspect of the chip and is the component that the mechanical testing focused on. The aim of this testing is to determine whether the design and the valve in particular will fit the use-case for which it was designed, namely an experiment where the valve can stay closed for several hours and be opened and closed a few times. Additionally, the goal is to determine what flow rates can be used during experiments.

Firstly, the valve was able to reversibly open and close as can be seen in Figure 4.10. The valve was actuated using a hex key while the device was filled with ink to visualize the fluid being able to pass or being blocked. The valve was operated upwards of 15 times without failure. It did, however, show small tears in the PDMS around the embedded bolt after testing.

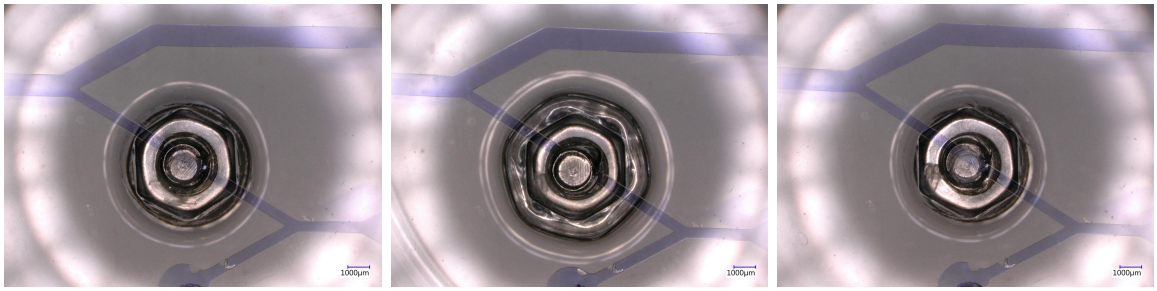

(a) (b) (c)

Figure 4.10: View of the screw valve from the underside of the chip. The valve is open in 4.10a, closed in 4.10b, and opened again in 4.10c as can be seen from the ink moving under the end of the bolt.

The testing of the valve under flow was performed by applying flows between 10μL/min to 5mL/min using a syringe pump. Ink was flowed through the chip from the cell chamber at different rates in open and in closed state as is shown in Figures 4.11 and 4.12. In Figure 4.11 the chip is filled with a mixture of water and ink from right to left. One can see the ink diffusing into the water slightly in Figure 4.11a. The ink was flowed-in via the cell culture chamber and fills the larger main channel and only then goes through the side channel. This is caused by the difference in microfluidic resistance. Since this channel is larger the mirofluidic resistance is lower. As described by equation 2.7 in section 3.2, the resistance is a function of

the dimension of the channel. In this case, the wide channel is twice as wide as the narrow channel and approximately the same length:

$$R_{wide} = \frac{1}{1 - 0.63(h/2w)} \frac{12\mu L}{h^3 2w} \tag{4.1}$$

$$R_{narrow} = \frac{1}{1 - 0.63(h/w)} \frac{12\mu L}{h^3 w} \tag{4.2}$$

$$R_{narrow}/R_{wide} = \frac{0.63h}{w - 0.63h} + 2 = 2.19 > 1 \tag{4.3}$$

Thus the resistance is more that twice as large in the smaller channel, which means the fluid flows at a larger rate in the main channel than into the side one. This helps prevent leakages when the flow to the biosensor chamber is not desired.

In the case of a closed valve as seen in Figure 4.12, the flow never entered the side channel to the biosensor chamber. As can be seen in Table 4.2, no failure occurred during testing. For all tested flow rates the valve performed as desired in both open and closed states. The only failure observed occurred when water was flowed very forcefully through the chip by hand using a syringe. The failure point in this instance was a tear in the PDMS in the side of the cell culture chamber and not the valve.

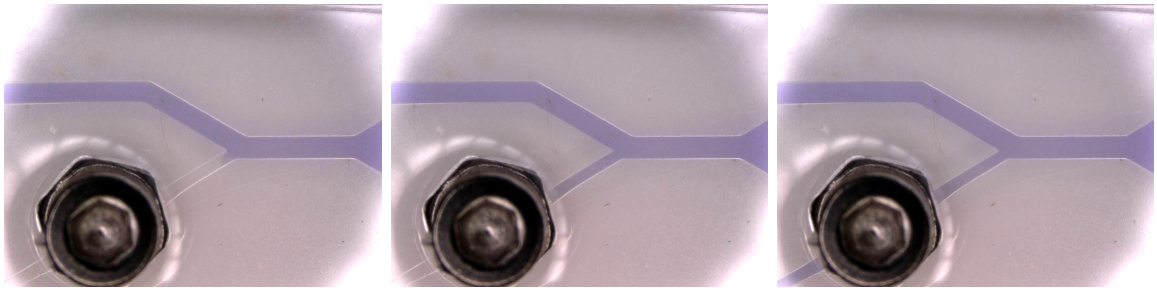

(a) (b) (c)

Figure 4.11: Top view of the mechanical testing of the screw valve in open state. The ink flows from right to left in the side channel and through the valve to the sensor chamber.

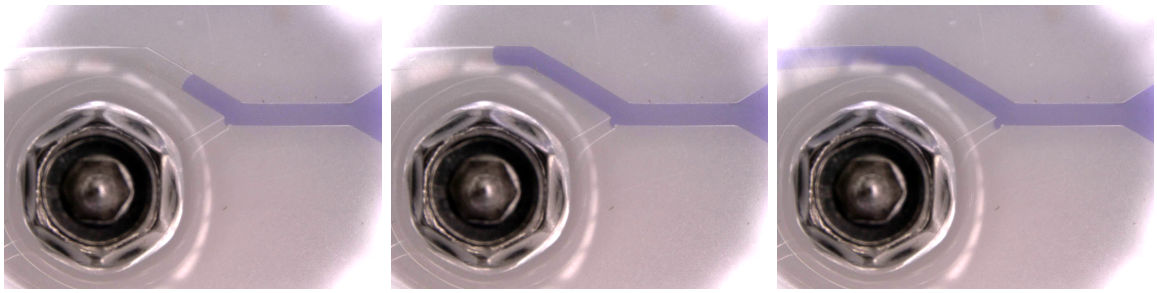

(a) (b) (c)

Figure 4.12: Top view of the mechanical testing of the screw valve in closed state. The ink never flows from right to left in the side channel and remains in the wider channel.

Flow rate μL/min	Fail (x) or Success (✓)
10	✓
15	✓
20	✓
50	✓
100	✓
500	✓
5000	✓

Table 4.2: Results of the mechanical testing for different flow rates of the screw valve inside the microfluidic chip.

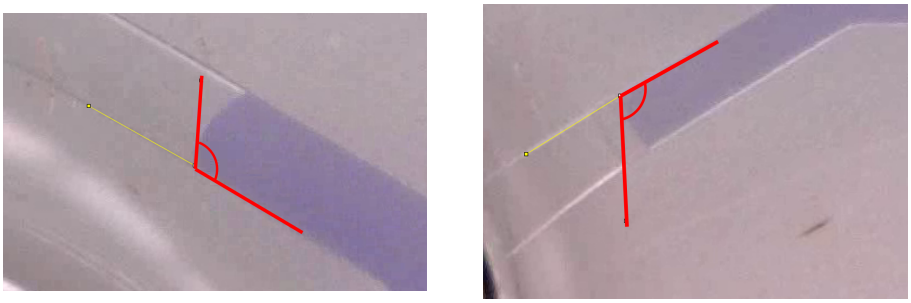

(a) (b)

Figure 4.13: Front of the water entering the channels in the microfluidic device in the wide (1mm) channel 4.13a and the narrow channel (500μm) 4.13b

Figure 4.13, shows the liquid front as it progressed in the channels. The angle between the wall of the channel and the liquid was measured to be around 120°±5 in these images. As described by equation 2.10 in section 3.2. The capillary pressure caused by this interaction is:

$$\Delta P_c = -2\sigma(\frac{cos\theta_w}{w} + \frac{cos\theta_h}{h}) \tag{4.4}$$

Here since $cos(120^o) = -0.5$, the capillary front acts as a pressure barrier for the liquid. In this case in both the narrow and wide channel have the same height. Thus the difference in pressure in both channels is:

$$\Delta P_{w\&n} = -2\sigma(\frac{cos\theta_w}{w_{small}} + \frac{cos\theta_h}{h} - \frac{cos\theta_w}{w_{big}} - \frac{cos\theta_h}{h}) = -2\sigma(\frac{cos\theta_w}{w_{small}} - \frac{cos\theta_w}{w_{big}}) \tag{4.5}$$

$$\Delta P_{w\&n} = \sigma(\frac{1}{w_{small}} - \frac{1}{2w_{small}}) = \sigma\frac{1}{2w_{small}} \simeq 72.8Pa > 0 \tag{4.6}$$

Which means that higher pressure is needed to push flow in the more narrow side channel leading to the sensor chamber compared to the wider channel.

Discussion As discussed above, this valve design performed well. The design including a narrower sampling channel was able to contribute to the valve being leak proof when the

valve is closed. During experiments it was also confirmed that cells were not able to grow past the valve when it is closed.
Furthermore, as described above, the capillary pressure must be overcome for the channel leading to the biosensor to be filled. Once the whole chip is full of fluid, which is the case when experiments take place after the cell culture is already seeded, the narrow channel is still the path of higher resistance. Thus liquid only flows at a smaller rate through this channel, which helps in keeping the valve leak proof. In this experiment this pressure was caused by the main channel being filled with liquid. This can, however, also be achieved by either pinching the tubing from the main channel outlet or simply plugging it. During subsequent experiments a plug was fabricated by curing glue inside a syringe tip that was used to this effect.

From the results is can be concluded that the valve design does fit the use case of this project. The end goal for this device is to be used in an experiment in which the cells are seeded in the chip when the valve is closed, followed by overnight incubation and then, the next morning, stimulated and the medium analyzed. During this experiment the valve is actuated infrequently and left a long period of time in an incubator without access to actuation equipment such as pressurized air or an electric source. Additionally, no limitation in flow rate is necessary, since the valve did not fail during testing. Preliminary experiments can thus be executed by pipetting, instead of using syringe pumps, without fearing breaking the seal of the valve. As such the compact device with manual actuation, that remains in its open or closed position, is a good solution that matches the requirements in this experiment.
This design of screw valve using a prefabricated nut and bolt compares to similar examples in literature. Although different fabrication methods are used in literature [43], [42], the screw valves in this project generally presented similar advantages. They are relatively easy and inexpensive to fabricate, do not depend on large external equipment such as compressed air systems or electronic actuation, and allow easy manual actuation by the user. This type of valve is suited to uses in scenarios where a valve will be used in the range of around 10 to 20 times where automated actuation is not necessary or possible and a simple chip design where two or more compartments need to be separated temporarily

4.2.2 Viability testing

A second characteristic that the chip needed to be tested for is its bio-compatibility. Moreover, it is important to compare the viability of the cells in the well plates, the cell culture environment of the first experiment described in section 4.1, to the viability of the cells in the microfluidic chip to form a correct expectation of the possible IL-6 concentration. The adequacy of the chip to host cells was determined by the use of a viability assay as described in section 3.1.

An example of the resulting images is shown in Figure 4.14. The cells have been imaged after overnight incubation and stained the next morning in order to keep the protocol the same as with the IL-6 measurement experiments. Figure 4.14a presents an example of a typical view of the "live" cell stain, which stains all cell nuclei, both alive and dead. Figure 4.14b, shows a typical example of the "dead" cell stain, which only stains dead cells, on the same area. Figure 4.15, a composite image of both the "live" and "dead" stain, gives a first impression of the proportion of live cells. In all images taken, including Figure 4.15, the live cells were the overwhelming majority. Overall the viability of the cell was very high and

comparable to cells cultured inside a typical 24-well plate. As can be seen in table 4.3, in all cases the viability was above 97%.

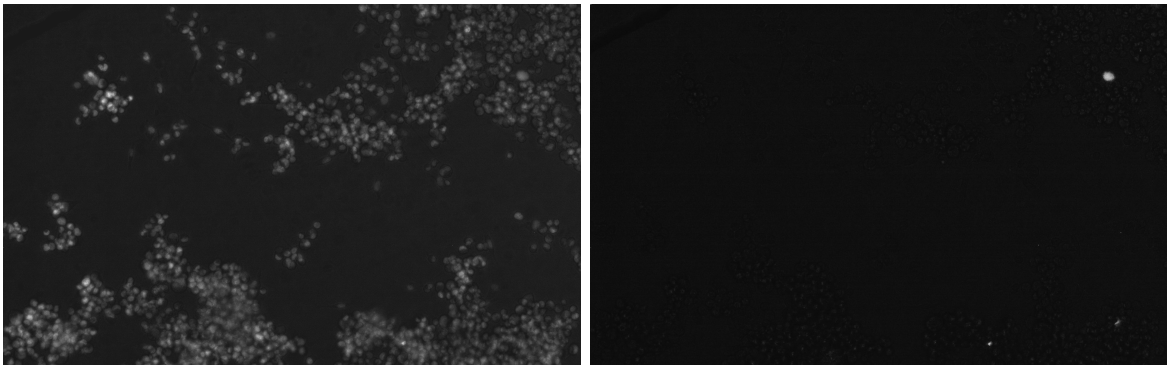

(a) (b)

Figure 4.14: Images of a live/dead cell viability staining experiment of $1400 \cdot 10^4$ MDA MB 231 cells/mL inside the cell chamber of the microfluidic chip. The stain in 4.14a stains all cell nuclei, and the stain in 4.14b only stains dead cells.

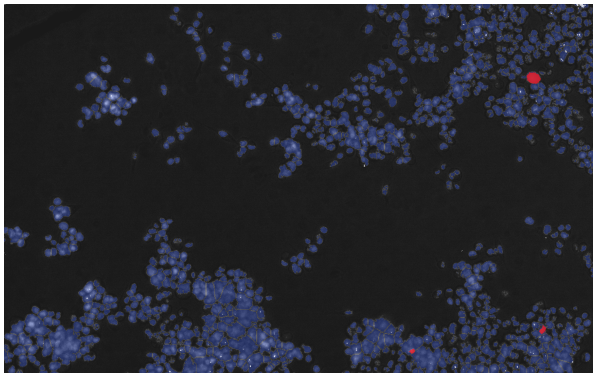

Figure 4.15: Composite image of a live/dead cell viability staining experiment of $1400 \cdot 10^4$ MDA MB 231 cells/mL inside the cell chamber of the microfluidic chip.
The cells in blue are stained with the "live" cell stain, and the cells in read are stained with the "dead" cell stain. The live cells make up the large majority of the cells in this image.

	Cell density in 10^4cells/mL	Cell type	Viability
24 well-plate	7	MCF 7	99,2±0,3%
24 well-plate	7	MDA MB 231	98,7±0,2%
microfluidic chip	140	MDA MB 231	99,4±0,2%
microfluidic chip	1400	MCF 7	97,7±0,6%
microfluidic chip	1400	MDA MB 231	99,4±0,1%

Table 4.3: Results of the viability testing via live/dead staining in the microfluidic chip compared to the well plate

Discussion As can be understood from the results presented in Table 4.3 the viability of the MDA MB 231 cells in the well plate is comparable to that of the cells in the microfluidic chip. This indicates two things. First, it confirms that the microfluidic environment is adequate for cell culture, which means the cells should behave in a similar way as in a well plate and thus produce IL-6 at a similar rate. This leads to the assumption that the IL-6 concentration could be linearly scaled with the cell density. This hypothesis is tested in following experiments.

The error in the viability is caused by the processing of the captured images. As described in section 3.1, the cells were counted in black and white images by using a particle counting software with a brightness threshold in Image J. The resulting total cell count is very sensitive to this threshold. If the threshold is too low some cells in the image are below the threshold and thus left out of the count. If the threshold is too high some background is included in the cell count. The threshold was chosen by observing the image at different thresholds and making sure the visible cells in the original image are included in the count. However, after analyzing a sample image with a known cell count, the range of threshold that seem empirically correct leads to an error of almost 20% in the number of total counted cells. Nevertheless, the viability is calculated as follows $Viability = 1 - N_{dead}/N_{totalcells}$, with $N_{dead} << N_{totalcells}$. Thus, the relative error in total cell count is of only small impact for the error in viability.

Cell viabilities between 80-100% [38], [39], [40], are considered adequate. Thus, in all these cases the cell culture is easily considered viable. Additionally, the resulting viability in the microfluidic chip was found to be the same as the viability in the well plate. Thus, no difference in behavior is expected. These results confirm that the microfluidic environment and the used protocol are adequate for cell stimulation.

4.3 Preliminary work on a fluorescent biosensor

After determining the rate of IL-6 production per cell and confirming the adequacy of the device to host the desired experiment, the next step was to integrate the biosensor into the microfluidic chip. Firstly the sensitivity of the method and setup was determined, to evaluate whether it is suitable. The estimated IL-6 concentration for $1400{\cdot}10^4$ cells/mL stimulated MDA MB 231 cells after 3 hours of incubation is estimated to 10500 pg/mL or 500 pM, by multiplying the result of 2.5pg/hour/10^4 cells of the experiment in section 4.1. This was thus the minimum targeted range for the LOD of the detection method.

The experiment was performed as described in sec 3.1. The optical setup used is a wide-field epifluorescent microscope with a filter cube including filters and a dichroic mirror. The brightness of a monolayer of fluorophores was plotted against the concentration. The resulting curves for different numerical apertures and exposures times were plotted in Figure 4.16, 4.17, 4.18. From these curves the resulting LOD and LOQ were calculated as described in section 3.1, the results of which are shown in Table 4.4.

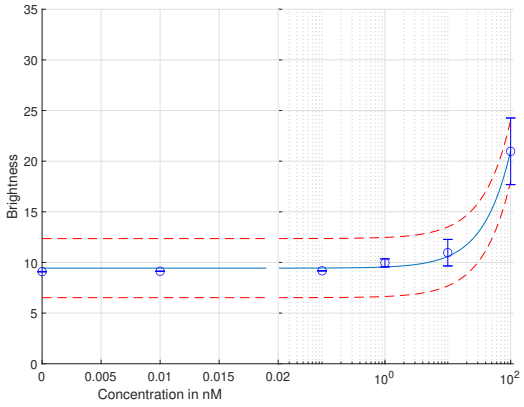

Figure 4.16: Image brightness as a function of fluorophore concentration from a monolayer with a 20x dry objective and a shutter time of 41ms

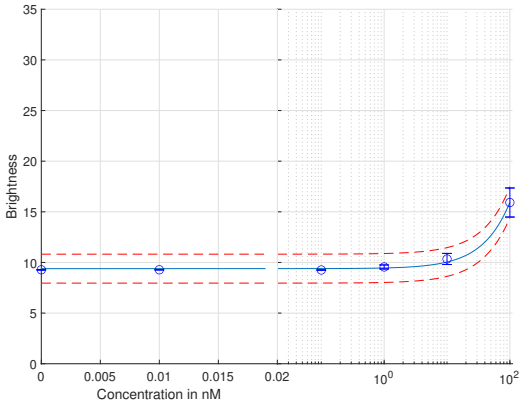

Figure 4.17: Image brightness as a function of fluorophore concentration from a monolayer with a 20x dry objective and a shutter time of 100ms

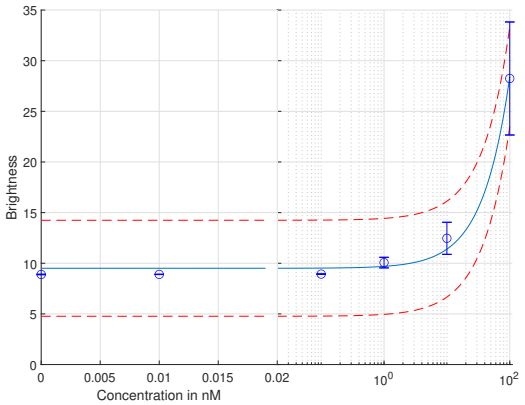

Figure 4.18: Image brightness as a function of fluorophore concentration from a monolayer with a 63x water immersion objective and a shutter time of 100ms

Shutter time (ms)	Objective	NA	LOD (nM)	LOQ (nM)
41	20x	0.4	5,2 ± 0,2	17,5 ± 0,8
100	20x	0.4	8,4 ± 0,5	27,8 ± 1,7
100	63x	0.9	5,2 ± 0,2	17,3 ± 0,8

Table 4.4: Calculated LOD based on the curve obtained from an experiment with monolayers of fluorophore of know concentrations using different objectives and shutter times.

Discussion The calculated LOD does is higher than the required 500pM sensitivity, and, as can be seen in Table 4.4, a longer shutter time did not improve the LOD. This is unexpected because for a longer shutter time, the amount of photons that reach the sensor should

be larger. A possible explanation for this could be that since the measurements for longer shutter times were done later in the experiment the fluorophores were already partially photobleached.

Furthermore, changing to a higher NA objective did not yield a much lower LOD. Although, the higher NA did improve the LOD somewhat, the improvement is not sufficient to bridge a gap of one order of magnitude to the desired LOD. Moreover, this result could also be influenced by photobleaching that was obvserved at this point in the experiment, or user error in finding the focus plane while using an objective with a much shorter depth of field.

As seen in Table 4.4, the LOD attained with this setup was around 5nM, and thus, an improvement of only one order of magnitude is necessary to reach the desired range of 500pM. A possible component that could improve the sensitivity is the camera used to capture the images of the fluorescence. The camera used in this setup has an absolute sensitivity threshold, the average number of photons required to get a a signal equal to noise [48], of 18.67 γ [49]. Large improvements can be made by using a more sensitive camera. There are small cameras with a sensor with an absolute sensitivity threshold of 3.51 [50], and larger specialized cameras with single photon sensitivity [51] thanks to CMOS amplifiers. Additionally, the quantum efficiency of the used sensor was quite low (under 50% [52]) for the desired range of 600-700nm. Furthermore, from Figures 4.16 4.17 4.18, it seems that all captured images at blank have a similar, non-temporal, noise for a dark image. This noise remains the same for longer shutter times. Consequently, the most straightforward improvement to this setup to increase the sensitivity by one order of magnitude is to simply swap the camera for a more sensitive one, and match the peak in fluorescent emission to the peak in quantum efficiency of the sensor. This is the main recommendation to improve the device function in further research.
Other imaging techniques such as TIRF or confocal microscopy, which are capable of single molecule sensitivity could also be used in place of wide-field epifluorescent microscopy. In our case, the ratio of noise to signal is too high for lower concentrations and does not permit the distinction of signal. However, the added complexity is a disadvantage of switching to such a setup. Another option would be to use a different transducer technique than fluorescence. Beads could be used as marker for instance.[7][27] Additionally, for a sIFA, optimization of the protocol regarding incubation times and blocking steps for instance should be taken.

Another important consideration is the need for a standard. In the experiments performed so far the standard concentrations were either prepared on a number of microfluidic chips, or on several microscope slides or coverslips. This aspect could be included in a future version of the design or a companion chip that would go alongside the experiment. This standard chip could be prepared with the same protocol of the sample sensor chamber, being pre-coated in capture antibodies beforehand. A second chamber, with prepared standard solutions of antigen, detection antibody and fluorophores complexes could then be opened at the same time as the sample is introduced in the sample chip. Thus, similarly to commercial ELISAs, for every experiment a standard is processed at the same time to ensure reliable results.

4.4 Validating IL-6 production in microfluidic environment

To validate the estimated concentration of about 500pM, or 10500pg/mL, IL-6 produced by stimulated MDA MB 231 cells inside a microfluidics chip, a high concentration of cells was seeded inside the microfluidic chip and the IL-6 was analyzed off-chip using an amplified ELISA as described in section 3.1. The sample from the chips was diluted in order to have a sufficiently large sample volume for ELISA analysis as well as putting the expected concentration in the assay range. Thus, the results have been multiplied by the dilution factors to reflect the IL-6 concentration inside the microfluidic chip.

The results of the experiment in the chip are shown in Figure 4.19. The concentration of IL-6 after 3 hour of incubation with and without stimulation using TNF-α were measured for MCF 7 and MDA MB 231 cells. As with previous experiments control experiment with MCF 7 were performed but all results were below the detection limit. These results are normalized to 10^5 cells/mL (divided by 140 for $1400{\cdot}10^4$ cells, and by 7/10 for $7{\cdot}10^4$) to be able to compared them to previous results of experiments 1 and 3 performed in the well plate, shown in Figure 4.20 and 4.21.

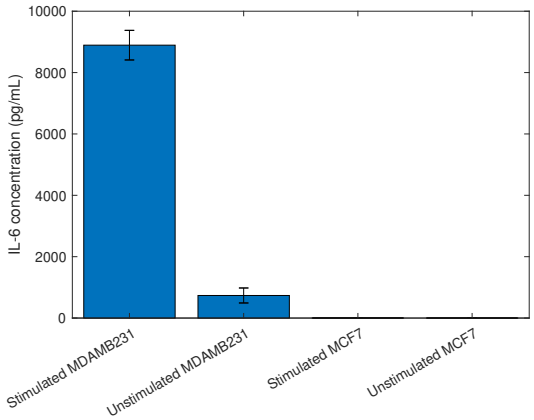

Figure 4.19: IL-6 concentration in pg/mL produced by stimulated (TNF-α 10 ng/mL) and unstimulated MDA MB 231 and MCF 7cells ($1400 \cdot 10^4$cells/mL) during an incubation time of 3 hours inside the microfluidic chip.

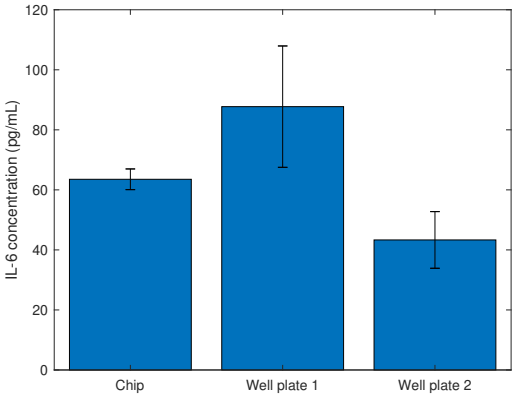

Figure 4.20: IL-6 concentration in pg/mL produced by stimulated (TNF-α 10 ng/mL) MDA MB 231 cells normalized to 10^5 during an incubation time of 3 hours inside the microfluidic chip compared to experiments performed in a well plate.

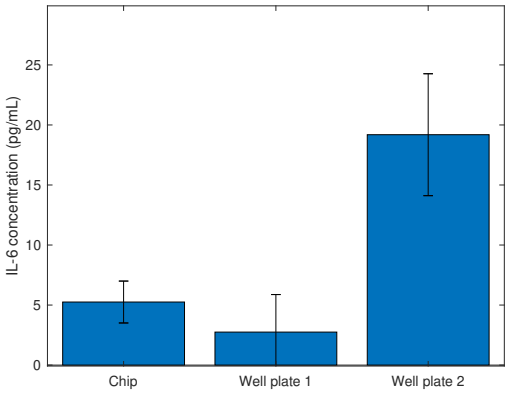

Figure 4.21: IL-6 concentration in pg/mL produced by unstimulated MDA MB 231 cells normalized to 10^5 during an incubation time of 3 hours inside the microfluidic chip compared to experiments performed in a well plate.

Discussion As can be seen in Figure 4.19, the IL-6 concentration after 3 hours of incubation of stimulated MDA MB 231 cells, was just under the predicted value of 10500 pg/mL, the actual value is 9376 $\pm$ 980 pg/mL. However, as can be seen in Figure4.20, the normalized results agree very well with the results from experiment 1, were the cell line was youngest. The same can be said for the unstimulated MBA MB 231 cells, as is shown in Figure 4.21. This does support the hypothesis that the IL-6 concentration scales linearly with the cell density in a given volume. Additionally, these results show that the microfluidic chip can be a suitable environment to succesfully perform stimulation experiments of these breast cancer cells. For future experiments, testing the IL-6 production in a more physiologically relevant environment by creating a 3D cell culture, and comparing this production rate to the one measured here would be the next step after a fully functioning integrated biosensor.

The production rate calculated from the results obtained here can be used to slightly adjust the desired assay range for the biosensor. The LOD should be lowered from 500pM to approximatly 450pM for a stimulation time of 3 hours. The previous recommendation of changing the camera to gain sensitivity remains and should still be sufficient to improve the sensitivty eleven-fold instead of ten-fold. Especially in the case of a single photon sensitive camera, since this would represent an approximate twenty-fold improvement.

5 Conclusion

The aim of this project was to develop a microfluidic device incorporating a cell culture and a biosensor in order to observe the behaviour of triple negative breast cancer cells as a result of TNF-α stimulation by measuring IL-6 production.

First, the IL-6 produced as a result of 10 ng/mL of TNF-α stimulation in traditional cell culture vessels was determined. The basal production rate of MDA MB 231 cells was found to be 0,7 pg/hour/10^4cells for unstimulated cells. Upon stimulation the production rate increased to 2,5 pg/hour/10^4cells. These results are in accordance with literature. Additionally, control experiments with MCF 7 cells were performed and no detectable IL-6 was found. Next, the prototype of the microfluidic device was tested to evaluate its mechanical properties. The valve of the device was determined to perform well for flows ranging from 10 μL/min to 5 mL/min. The bolt-nut valve developed here is particularly well suited to use-cases where it will be actuated up to 20 times and where automated actuation is not necessary or possible. In addition, the cell viability was confirmed to be very high, above 97 %, inside the microfluidic device. Subsequently, the sensitivity of a potential integrated fluorescent biosensor was tested. The limit of detection was determined to be 5$\pm$ 0,2 nM, which is not sufficient to measure the produced IL-6 concentration range in a chip, which is around 450pM, implying that the optical setup is not sensitive enough. Finally, the production of IL-6 inside the microfluidic device was tested off-chip and found to be in accordance with prior experiments in well plates for the case of cell with low passage counts.

Some recommendations can be made for further research. First, to prevent reproducibility problems, cell cultures with low passage count should be used. Methods to achieve homogeneous and precise cell counts upon seeding, such as automated cell counting are also recommended. To improve the sensitivity of the sensor, the optical setup should be optimized. In particular, a camera with a high sensitivity should be used. Additionally, the biochemical protocol should be optimized, interms of incubation times and blocking steps, which can be done using a complex matrix produced with the help of MCF 7 cells. Finally, it would be valuable to introduce a 3D cell culture in the microfluidic device to improve upon the physiological relevance of the model, and compare with the results presented here.

Overall, the results of the designed chip are promising. From these results a functioning device within the realm of experimental possibilities, after the implementation of the recommendations. However, a limitation of sandwich assays is the fact that the integrated sensor is not continuous. The advantages of the chip in both research and clinical settings would be greater if a continuous biosensor, such as BPM [7], would be implemented since the time elapsed between experiment and obtaining the result would be greatly reduced. Aside from this limitation, this device and similar devices, could be used in cancer research to screen drugs or model disease. For instance, the level of inflammation for different treatments could be observed. This device could also be used as a platform for personalized medicine. On the whole, this project fits into the emerging trend of biosensor integration [3] in advanced microfluidic cell culture devices in order to enhance device functionality.

References

[1] M. Mehling and S. Tay, "Microfluidic cell culture," *Current Opinion in Biotechnology*, vol. 25, pp. 95–102, 2014.

[2] M. Rothbauer and P. Ertl, "Emerging Biosensor Trends in Organ-on-a-Chip," 2020.

[3] S. R. Adam Kratz, G. Höll, P. Schuller, P. Ertl, and M. Rothbauer, "Latest trends in biosensing for microphysiological organs-on-a-chip and body-on-a-chip systems," *Biosensors*, vol. 9, no. 3, 2019.

[4] L. Faggioli, C. Costanzo, M. Merola, E. Bianchini, A. Furia, A. Carsana, and M. Palmieri, "Nuclear factor κB (NF-κB), nuclear factor interleukin-6 (NFIL-6 or C/EBPβ) and nuclear factor interleukin-6β (NFIL6-β or C/EBPδ) are not sufficient to activate the endogenous interleukin-6 gene in the human breast-carcinoma cell line MCF-7. Comparative an," *European Journal of Biochemistry*, vol. 239, no. 3, pp. 624–631, 1996.

[5] C. Suarez-Cuervo, K. W. Harris, L. Kallman, H. K. Väänänen, and K. S. Selander, "Tumor necrosis factor-α induces interleukin-6 production via extracellular-regulated kinase 1 activation in breast cancer cells," *Breast Cancer Research and Treatment*, vol. 80, no. 1, pp. 71–78, 2003.

[6] A. M. Schrell, N. Mukhitov, L. Yi, X. Wang, and M. G. Roper, "Microfluidic Devices for the Measurement of Cellular Secretion," *Annual Review of Analytical Chemistry*, vol. 9, no. June, pp. 249–269, 2016.

[7] E. W. Visser, J. Yan, L. J. Van IJzendoorn, and M. W. Prins, "Continuous biomarker monitoring by particle mobility sensing with single molecule resolution," *Nature Communications*, vol. 9, no. 1, pp. 1–10, 2018. [Online]. Available: http://dx.doi.org/10.1038/s41467-018-04802-8

[8] Cancer Research UK, "Triple negative breast cancer," 2021. [Online]. Available: https://www.cancerresearchuk.org/about-cancer/breast-cancer/stages-types-grades/types/triple-negative-breast-cancer

[9] L. Faggioli, C. Costanzo, M. Merola, E. Bianchini, A. Furia, A. Carsana, and M. Palmieri, "Nuclear factor κB (NF-κB), nuclear factor interleukin-6 (NFIL-6 or C/EBPβ) and nuclear factor interleukin-6β (NFIL6-β or C/EBPδ) are not sufficient to activate the endogenous interleukin-6 gene in the human breast-carcinoma cell line MCF-7. Comparative an," *European Journal of Biochemistry*, vol. 239, no. 3, pp. 624–631, 1996.

[10] G. Sittampalam, N. Coussens, M. Arkin, D. Auld, C. Austin, B. Bejcek, M. Glicksman, J. Inglese, P. Iversen, J. Mcgee, O. Mcmanus, L. Minor, A. Napper, J. M. Peltier, T. Riss, O. Trask, and J. Weidner, "Assay Guidance Manual," *Assay Guidance Manual*, no. Md, pp. 305–336, 2016.

[11] K. L. Cox, "Immunoassay Development, Optimization and Validation Flow Chart," *ImmunoAssay Methods*, no. Md, pp. 1–38, 2011.

[12] R. Pörtner, U. Jandt, and A. P. Zeng, *Cell culture technology*, 2016.

[13] J. Cooper, "Cell line profile A549," *European Collection of Authenticated Cell Cultures*, vol. 7, no. 86012803, pp. 1–2, 2012.

[14] European College of Authenticated Cell cultures, "Cell line profile MDA-MB-231," *European Collection of Authenticated Cell Cultures*, vol. 231, no. 92020424, pp. 1–3, 2017. [Online]. Available: https://www.phe-culturecollections.org.uk/media/133182/mda-mb-231-cell-line-profile.pdf

[15] J. Sleeboom, C. Sahlgren, and J. den Toonder, "Cancer stem cell migration in an oxygen gradient characterized using a microfluidic device," *22nd International Conference on Miniaturized Systems for Chemistry and Life Sciences*, vol. 3, pp. 1517–1520, 2018.

[16] H. H. Lee, J. Jung, A. Moon, H. Kang, and H. Cho, "Antitumor and anti-invasive effect of apigenin on human breast carcinoma through suppression of IL-6 expression," *International Journal of Molecular Sciences*, vol. 20, no. 13, 2019.

[17] M. A. Khan and M. Mujahid, "Recent advances in electrochemical and optical biosensors designed for detection of Interleukin 6," *Sensors (Switzerland)*, vol. 20, no. 3, pp. 1–27, 2020.

[18] Y. Pylayeva-Gupta, "Fundemental of Cell Culturing in Microfludiic Devices," *Bone*, vol. 23, no. 1, pp. 1–7, 2011.

[19] Y. Xiao, B. Zhang, A. Hsieh, N. Thavandiran, C. Martin, and M. Radisic, *Microfluidic Cell Culture Techniques*, first edit ed. Elsevier Inc., 2012. [Online]. Available: http://dx.doi.org/10.1016/B978-1-4377-3459-1.00012-0

[20] M. R. Bennett, W. L. Pang, N. A. Ostroff, B. L. Baumgartner, S. Nayak, L. S. Tsimring, and J. Hasty, "Metabolic gene regulation in a dynamically changing environment," *Nature*, vol. 454, no. 7208, pp. 1119–1122, 2008.

[21] Y. A. Chen, A. D. King, H. C. Shih, C. C. Peng, C. Y. Wu, W. H. Liao, and Y. C. Tung, "Generation of oxygen gradients in microfluidic devices for cell culture using spatially confined chemical reactions," *Lab on a Chip*, vol. 11, no. 21, pp. 3626–3633, 2011.

[22] F. Kurth, E. Györvary, S. Heub, D. Ledroit, S. Paoletti, K. Renggli, V. Revol, M. Verhulsel, G. Weder, and F. Loizeau, *Organs-on-a-chip engineering*, 2019.

[23] J. M. Wilkinson, *Need for alternative testing methods and opportunities for organ-on-a-chip systems*. Elsevier Inc., 2020. [Online]. Available: http://dx.doi.org/10.1016/B978-0-12-817202-5.00001-2

[24] A. Van Den Berg, C. L. Mummery, R. Passier, and A. D. Van der Meer, "Personalised organs-on-chips: functional testing for precision medicine," *Lab on a Chip*, vol. 19, no. 2, pp. 198–205, 2019.

[25] D. Wartmann, M. Rothbauer, O. Kuten, C. Barresi, C. Visus, T. Felzmann, and P. Ertl, "Automated, miniaturized, and integrated quality control-on-chip (QC-on-a-chip) for cell-based cancer therapy applications," *Frontiers in Materials*, vol. 2, no. September, 2015.

[26] X. Li, M. Soler, C. Szydzik, K. Khoshmanesh, J. Schmidt, G. Coukos, A. Mitchell, and H. Altug, "Label-Free Optofluidic Nanobiosensor Enables Real-Time Analysis of Single-Cell Cytokine Secretion," *Small*, vol. 14, no. 26, pp. 1–11, 2018.

[27] K. J. Son, P. Gheibi, G. Stybayeva, A. Rahimian, and A. Revzin, "Detecting cell-secreted growth factors in microfluidic devices using bead-based biosensors," *Microsystems and Nanoengineering*, vol. 3, no. July 2016, pp. 1–9, 2017. [Online]. Available: http://dx.doi.org/10.1038/micronano.2017.25

[28] D. A. Armbruster and T. Pry, "Limit of blank, limit of detection and limit of quantitation." *The Clinical biochemist. Reviews*, vol. 29 Suppl 1, no. August, pp. 49–52, 2008. [Online]. Available: http://www.ncbi.nlm.nih.gov/pubmed/18852857%0Ahttp://www.pubmedcentral.nih.gov/articlerender.fcgi?artid=PMC2556583

[29] P. P. Mondal and A. Diaspro, *Fundamentals of Fluorescence Microscopy*, 2014.

[30] H. Bruus, *Theoretical Microfluidics*, 1st ed. Oxford University Press, 2008. [Online]. Available: https://www.researchgate.net/publication/305689093_Theoretical_Microfluidics

[31] M. B. Standing, "CAPILLARY PRESSURE," in *Stanford lecture notes*, 1977, ch. 3. [Online]. Available: https://web.mst.edu/~numbere/cp/chapter3.htm

[32] H. Cho, H. Y. Kim, J. Y. Kang, and T. S. Kim, "How the capillary burst microvalve works," *Journal of Colloid and Interface Science*, vol. 306, no. 2, pp. 379–385, 2007.

[33] invitrogen, "Human IL-6 Instant ELISA Kit," *Thermo fisher scientific*, vol. 0, no. 30, pp. 0–5, 2020.

[34] ——, "Human IL-6 High Sensitivity ELISA," *Thermo fisher scientific*, vol. 0, no. 33, pp. 1–22, 2020.

[35] F. Xia, X. Zhang, X. Lou, and Q. Yuan, "Biosensors based on sandwich assays," *Biosensors Based on Sandwich Assays*, no. January, pp. 1–216, 2018.

[36] fischer scientific, "Invitrogen™ NucBlue™ Live ReadyProbes™ Reagent (Hoechst 33342)." [Online]. Available: https://www.fishersci.com/shop/products/molecular-probes-nucblue-live-readyprobes-reagent/R37605

[37] ThermoFischer, "Invitrogen™ Propidium Iodide Catalog number: P1304MP." [Online]. Available: https://www.thermofisher.com/order/catalog/product/P1304MP

[38] S. Kamiloglu, G. Sari, T. Ozdal, and E. Capanoglu, "Guidelines for cell viability assays," *Food Frontiers*, vol. 1, no. 3, pp. 332–349, 2020.

[39] D. Gilbert and O. Friedrich, *Cell Viability Assays ,Methods and Protocols*, 2017. [Online]. Available: http://www.springer.com/series/7651

[40] A. Iwasawa, M. Ayaki, and Y. Niwano, "Cell viability score (CVS) as a good indicator of critical concentration of benzalkonium chloride for toxicity in cultured ocular surface cell lines," *Regulatory Toxicology and Pharmacology*, vol. 66, no. 2, pp. 177–183, 2013. [Online]. Available: http://dx.doi.org/10.1016/j.yrtph.2013.03.014

[41] TELEDYNE PHOTOMETRICS, "Filters - Microscopy Basics," 2021. [Online]. Available: https://www.photometrics.com/learn/microscopy-basics/filters-3

[42] S. Elizabeth Hulme, S. S. Shevkoplyas, and G. M. Whitesides, "Incorporation of prefabricated screw, pneumatic, and solenoid valves into microfluidic devices," *Lab on a Chip*, vol. 9, no. 1, pp. 79–86, 2009.

[43] D. B. Weibel, M. Kruithof, S. Potenta, S. K. Sia, A. Lee, and G. M. Whitesides, "Torque-actuated valves for microfluidics," *Analytical Chemistry*, vol. 77, no. 15, pp. 4726–4733, 2005.

[44] L. Mazutis and J. Gilbert, "single cell analysis - Aquapel info," *Nat Protocol*, vol. 8, no. 5, pp. 870–891, 2014.

[45] H. M. Ji, V. Samper, Y. Chen, C. K. Heng, T. M. Lim, and L. Yobas, "Silicon-based microfilters for whole blood cell separation," *Biomedical Microdevices*, vol. 10, no. 2, pp. 251–257, 2008.

[46] L. Richard, E. C. Cox, R. H. Austin, and J. C. Sturm, "Continuous Particle Separation through Deterministic Lateral Displacement," *Science*, vol. 304, no. 5673, pp. 987–990, 2015.

[47] S. Choi and J. K. Park, "Continuous hydrophoretic separation and sizing of microparticles using slanted obstacles in a microchannel," *Lab on a Chip*, vol. 7, no. 7, pp. 890–897, 2007.

[48] "Standard for Characterization of Image Sensors and Cameras," *European Machine Vision Association*, no. 3, pp. 1–36, 2010.

[49] Point Grey, "Mono camera sensor review," 2014.

[50] FLIR Integrated Imaging Solutions, "EMVA 1288 IMAGING PERFORMANCE FLIR-BLACKFLY®S," pp. 2018–2019, 2019.

[51] Oxford Instruments, "Neo 5.5 sCMOS sepcification sheet," pp. 1–6, 2021.

[52] FLIR, "FLIR Grasshopper3 - Technical Reference," p. 163, 2017. [Online]. Available: https://www.ptgrey.com/support/downloads/10125/

A Experimental protocols

A.1 Protocol for seeding cells in a well plate

A cell passage, the detachment of the cells from their vessel in order to pass them to a new one, must first be performed to be able to seed the cells in a well plate. After this is done:

- Two samples of 10μL are taken from the remaining cells suspended in cell medium after cell passage to determine the concentration.
- The cell concentration is determined by using a Neubauer's chamber.
- The cells are centrifuged at 200 rcf for 5 minutes and the cell medium is taken out.
- The cells are diluted using cell medium to the desired concentration of $7 \cdot 10^4$ cells/mL.
- The cells are seeded into the 24 well plate.
- The well plate is placed in an incubator for overnight incubation.

A.2 Protocol for seeding cells in a microfluidic chip

First the chip is cleaned and disinfected to ensure a fitting environment for the cell culture.

- The chip is placed in the flow cabinet and UV lighting is left on for 15 min
- Rinse three times with 70% ethanol by flowing in 40μL.
- Rinse three times with sterile PBS by flowing in 40μL.
- The valve is closed with the use of a hex key.

Then the cell seeding resumes after having performed a cell passage.

- Two samples of 10μL are taken from the remaining cells suspended in cell medium after cell passage to determine the concentration.
- The cell concentration is determined by using a Neubauer's chamber.
- The cells are centrifuged at 200 rcf for 5 minutes and the cell medium is taken out.
- The cells are diluted using cell medium to the desired concentration of $1400 \cdot 10^4$ cells/mL.
- The cells are gently flowed in the microfluidic device while the valve is closed.
- The device is placed in an incubator for overnight incubation.

A.3 Protocol for quantifying IL-6 production of Breast cancer cells in a well plate using an ELISA

- Pipet old medium out of cell wells
- Rinse wells with sterile PBS
- Add fresh serum free cell medium + 10 ng/ml TNF-a
- Pipet out two samples of 50μL for time t = 0hours
- Perform instant ELISA protocol as per manufacturer instructions
- Pipet out two samples of 50μL for time t = 3hours
- Perform instant ELISA protocol as per manufacturer instructions
- Pipet out two samples of 50μL for time t = 6hours
- Perform instant ELISA protocol as per manufacturer instructions
- Pipet out two samples of 50μL for time t = 9hours
- Perform instant ELISA protocol as per manufacturer instructions

A.4 Protocol for quantifying IL-6 production of Breast cancer cells in a microfluidic chip using an ELISA

- Rinse three times with sterile PBS by very gently flowing in 40μL
- Flow in fresh serum free cell medium + 10 ng/ml TNF-a
- Pipet out a sample of 20μL for time t = 3hours
- Dilute this sample with 80μL PBS to bring the total volume to 100μL
- Samples are then further diluted to reach the assay range. This is a 60x dilution for unstimulated MDA MB 231 cells, 1260x for stimulated MDA MB 231 cells, and 10x for MCF 7 cells
- Perform high sensitivity ELISA protocol as per manufacturer instructions

A.5 Protocol for Instant ELISA

A summary of the protocol for instant ELISA used in the experiment with stimulated cells in well plates is given here. For more detailed instructions one should consult the protocol provided by the manufacturer of the ELISA kit.

As seen in Figures A.1, A.2, and A.3, one of the ELISA kits used in this work was a pre-prepared kit that contained all components in lyophilized form in the well strips. As such, some of the described steps in section 3 were able to be executed simultaneously. Samples are added to well already containing a capture antibody, a detection antibody conjugated with

biotin, and streptavidin-HRP complexes. Then, the TMB substrate is added. Finally, the reaction is stopped using an acid and the results are read using a multiwell platereader.

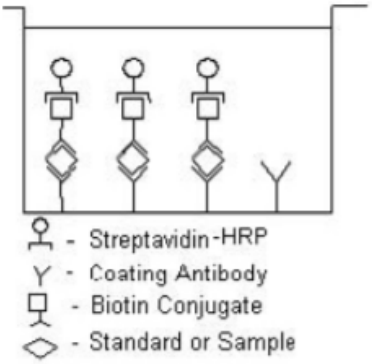

Figure A.1: Protocol for instant ELISA. Incubation 1: sample or standard incubated with lyophilized streptavidin-HRP and biotin conjugate[33]

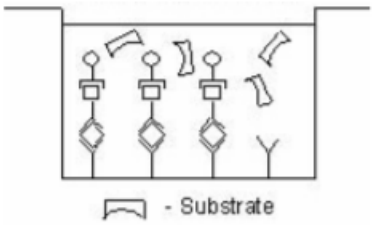

Figure A.2: Protocol for instant ELISA. Incubation 2: Incubate with TMB substrate until sufficient colored product has formed[33]

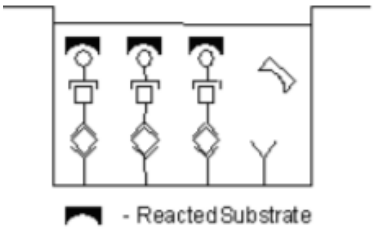

Figure A.3: Protocol for instant ELISA. Stop reaction: The reaction is terminated by the addition of acid and results can be read[33]

A.6 Protocol for High sensitivity ELISA

A summary of the protocol for high sensitivity ELISA used in the experiment with stimulated cells in the microfluidic device is given here. For more detailed instructions one should consult the protocol provided by the manufacturer of the ELISA kit.

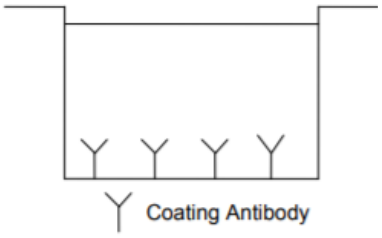

Figure A.4: Protocol for ELISA. Coated microwell: The microwell is coated in capture antibody [34]

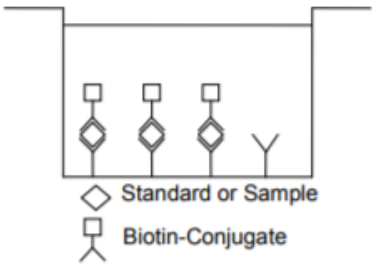

Figure A.5: Protocol for ELISA. Incubation 1: Samples and standards as well as Biotin conjugate is added to the wells[34]

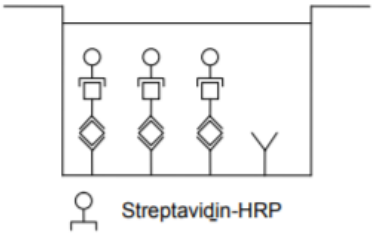

Figure A.6: Protocol for ELISA. Incubation 2: Incubate with streptavidin-HRP binding it to the biotin conjugates[34]

In this case the protocol of a typical ELISA is followed up until the addition of substrate, as can be seen in Figure A.7, A.8, and A.9. Instead of adding the substrate a amplification reagent, biotinyl-tyramide, is added to the wells. Next, after incubation, the second amplification reagent, more streptavidin-HRP, is introduced. Finally, the substrate is added and

the protocol resumes in the same manner as a typical ELISA.

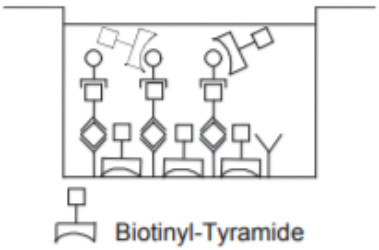

Figure A.7: Protocol for high sensitivity ELISA. Incubation 3: amplification reagent 1 (biotinyl-tyramide) is added[34]

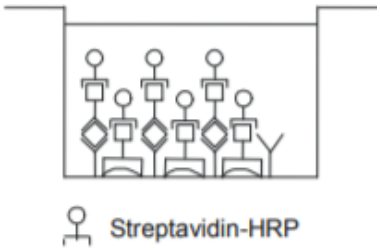

Figure A.8: Protocol for high sensitivity ELISA. Incubation 4: amplification reagent 1 (streptavidin-HRP) is added[34]

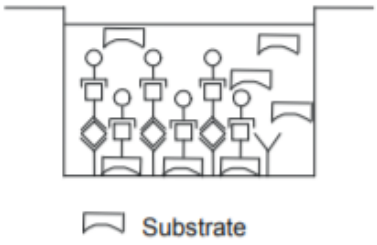

Figure A.9: Protocol for high sensitivity ELISA. Incubation 5: Incubate with TMB substrate until sufficient colored product has formed[34]

A.7 Protocol for preparing a silicon wafer for device moulding

- Clean dust of a silicon wafer with the use of nitrogen.
- Affix the wafer onto a spincoater.
- Pour approximately 4 to 5 mL of SU-8 2050 photoresist on the wafer.
- Spin at 500 rpm for 10 seconds with an acceleration of 100rpm/s.
- Spin at 500 rpm for 30 seconds with an acceleration of 300rpm/s.
- Soft bake. Place the wafer on a hot plate. Ramp the temperature of a hot plate up to 65^{o}C at a rate of 5^{o}C/min. Bake for 5 minutes. Then ramp the temperature the plate up to 95^{o}C at a rate of 5^{o}C/min. Bake for 30 minutes.
- Slowly cool the wafer down at a rate of 5^{o}C/min.
- Exposure. Place the photomask of top of the wafer. Expose the wafer for 15 seconds at 260 mJ/cm^2
- Post exposure bake. Place the wafer on a hot plate. Ramp the temperature of a hot plate up to 65^{o}C at a rate of 5^{o}C/min. Bake for 5 minutes. Then ramp the temperature the plate up to 95^{o}C at a rate of 5^{o}C/min. Bake for 12 minutes.
- Developing. Pour SU-8 developper in two petri dishes and agitate using an orbital shaker for 15min. When the developer in the first petri dish is saturated (around 10min), transfer the wafter to the second dish. After developing, rinse first with clean developer and then with IPA.
- Hard bake. Place the wafer on a hot plate. Ramp the temperature of a hot plate up to 120^{o}C at a rate of 5^{o}C/min. Bake for 30 minutes.

A.8 Protocol for molding a PDMS microfluidic chip using a silicon wafer

- Mix PDMS elastomer base and curing agent in a cup at a ratio of 10:1 by weight.
- Place in a desiccator and degas the PMDS mixture until all bubbles are gone.
- Clean dust of the wafer-mould using nitrogen.
- Create mould edges around the wafer using aluminium foil.
- Pour thin (1mm) PDMS layer on wafer mould.
- Place in desiccator to degas.
- Partially cure the PDMS in 20-25min at 65^oC.
- The next steps center om the creation of the valve in the device and are described below.

A.9 Protocol for fabricating a screw valve in a PDMS device

- Punch rings/disks out of a layer of cured PDMS of 1-2mm thick with an inner diameter the size of the thread on the bolt.
- Take the partially cured devices out of the oven.
- Carefully place the rings on top of the channel to be closed. In this case, the side channel to the sensor chamber, as can be seen in Figure A.10 and A.11.

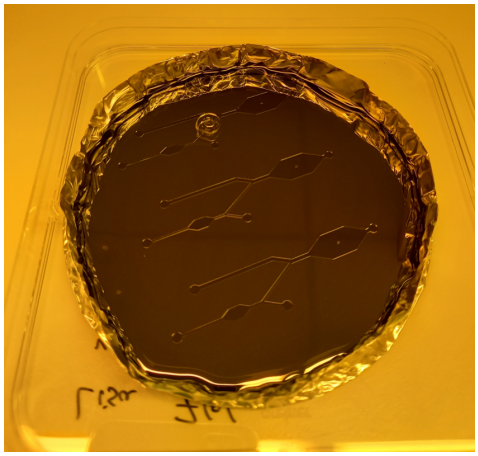

Figure A.10: PDMS ring placed on the side channel on partially cured device

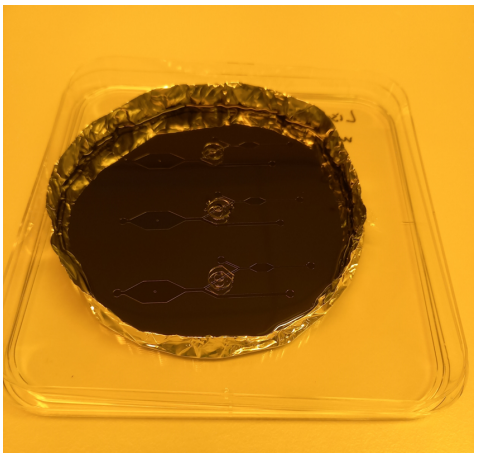

Figure A.11: PDMS rings placed on the side channel on partially cured devices

- Then place the bolt and nuts on these rings so that the thread that extends past the bolt has the same height as the rings. The result can be seen in Figure A.12.

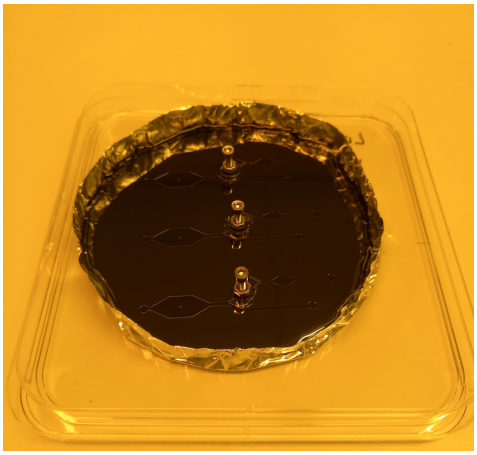

Figure A.12: Bolts and nuts rings placed on the side channel on partially cured devices in order to create a valve

- Pour PDMS over the devices so that the nuts are completly submerged.
- Degas the whole device carefully to remove all bubbles, as pictured in Figure A.13.

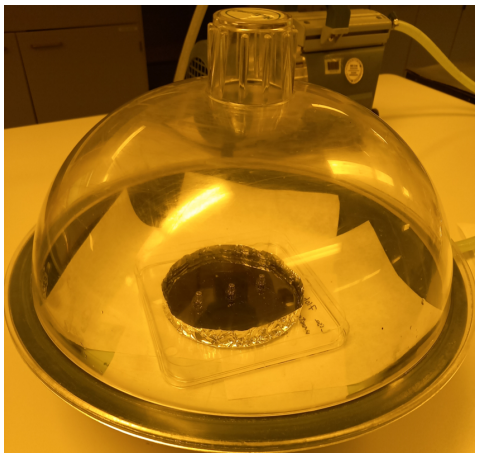

Figure A.13: Wafer mould with bolt/screw valve in desiccator in order to degas.

- Cure overnight in a 65^{o}C oven.

A.10 Protocol for functionalizing a biosensor chamber in a microfluidic device

Materials needed:

- Microfluidic device
- PBS
- Ethanol
- Isopropanol
- carbonate-bicarbonate coating buffer
- Blocking buffer (PBS 1% BSA)
- Wash buffer (PBS Tween-20)
- Capture IL-6 antibody, MQ2-13A5
- Detection antibody biotin conjugate MQ2-39C3
- Alexa Fluor 568-streptavidin
- IL-6 hydrolyzed protein

Clean and prepare the chip:

- Punch holes into the inlets and outlets of the microfluidic chip using the 1.2mm dermal punch
- Wash the whole chip using isopropanol. Each washing/rinsing step should be done by adding the volume of the chip 3 times (40uL whole chip 15uL side channel). Do not leave the isopropanol too long in the PDMS chip (it can make the plastic swell)

- Wash with ethanol
- Wash with PBS
- Mix antibodies in coating buffer, the goal is to have a solution with (100nMol with 150kDa) 15mg/mL
- In the second channel only, introduce the coating buffer with antibodies
- Let incubate for 2 hours at room temperature
- Wash with wash solution
- Rinse/wash with blocking solution
- Incubate for 30 min
- Wash with washing solution

In case standards are needed, prepare standards. 1nM was attempted in experiments of this project.

- Open the valve using hex key
- Close inlet number 1 using a stop
- Introduce the standard via inlet 1
- Incubate for 1 hour
- Wash
- Close valve
- Introduce detection solution number 1 (antibody) via inlet 2
- Incubate for 1 hour
- Wash
- Introduce detection solution number 2 (Alexa Fluor)
- Incubate in the dark for 30 min
- Wash
- Observe signal with microscope.

A.11 Protocol for functionalizing a glass surface with Alexa Fluor 568 fluorophores

The glass surface can be inside the fabricated microfluidic or a glass slide (with a chamber-sticker).

- clean the dust from the surface with nitrogen.
- Wash the surface with distilled water.
- Wash with ethanol.
- Dry
- Prepare a solution of PBS with Alexa Fluor 568-streptavidin at desired concencrations (10pM 100pM 1nM 10nM 100nM).
- Incubate for 2 hours at room temperature.
- Wash with distilled water.
- Image fluorescent signal on microscope.

B Error calculations

B.1 Error calculation in ELISA results

The error in the ELISA results is the sum of the variation between samples and the 2% precision in the signal specified by the manufacturer. The standrad-signal curve was fitted using a linear fit. With S signal, C concentration and a and b the parameters of the fit.

$$S = C * a + b \tag{B.1}$$

The error in the signal from the multiwell plate reader then causes an error in the concentration of.

$$e_m = 0.02 * S/a \tag{B.2}$$

The total error is then:

$$E_{ELISA} = e_m + \sigma \tag{B.3}$$

With σ, the standard deviation in the results form different samples.

B.2 Error calculation in cell viability assay

To estimate the error in the total cell count a representative sample image with known cell count was used. The chosen threshold chosen was varied to probe the behavior of the cell count. The result can be seen in Figure B.1. First, the threshold is too low to count any cells. Then, the brightest cells fall into the threshold, this is the beginning of the linear increase in cell count. Next, the background is captured and the cell count rises dramatically. Then, large areas of the background and cells are counted as a few cells and finally as only one.

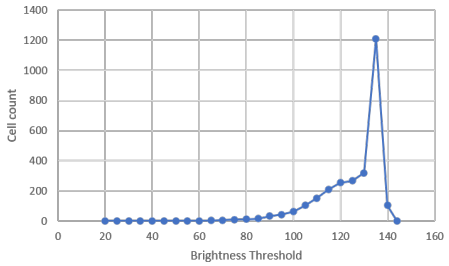

Figure B.1: Cell count as a function of brightness threshold of a representative sample image

The threshold was always chosen in the linear increase region, since it is quite obvious to the experimenter that a the threshold is wrong if it yields a result of only a few cells in an image containing a few hundred cells. The sensitivity of the cell count to the threshold is then estimated by a linear fit as pictured in Figure B.2.

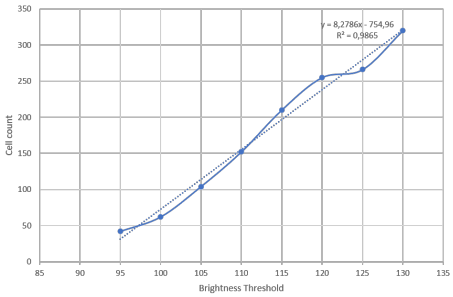

Figure B.2: Fitted cell count as a function of brightness threshold of a representative sample image

To then estimate the error in the cell count as a result of the slope (a_{cells}) of this fit, one needs to know the range of thresholds around the threshold that leads to the true count that is likely to be chosen. To determine the width of this range, a Gaussian fit was done over the difference between the cell count and the absolute difference to the cell count versus the threshold, shown in Figure B.3. The FWHM was found to about 11 threshold points. This range is matches with the range of threshold that seem empirically correct to an observer.

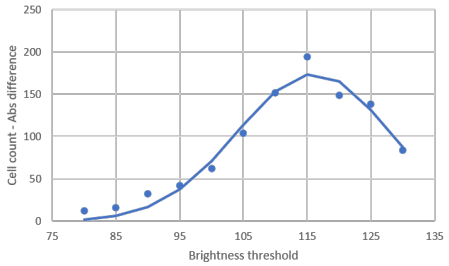

Figure B.3: Gaussian fit over the cell count as a function of brightness threshold of a representative sample image

Thus the relative error in the cell count is determined as follows.

$$E_{relativetotalcount} = (\frac{FWHM}{2} * a_{cells})/N_{cells} = 0.23 \tag{B.4}$$

With N_{cells} the true cell count. This should still be added to the standard deviation over different images in cell count σ, to determine the total error.

B.3 Error calculation in LOD and LOQ

The error in the LOD and LOQ is a result of the error in the linear fit.

$$S = c \cdot a + S_b \tag{B.5}$$

where S_{LOD} is the signal at the limit of detection, S_b is the signal at blank and $3\sigma_b$ is the standard deviation of this signal at blank. The error then is:

$$E_{LOD} = LOD * e_{slope}/a \tag{B.6}$$

Where e_{slope} is the error in the slope of the fit, and E_{LOD} the error in the LOD. Similarly for LOQ.

$$E_{LOQ} = LOQ * e_{slope}/a \tag{B.7}$$